Suppression of an Already Established Tumor Growing through Activated Mucosal CTLs Induced by Oral Administration of Tumor Antigen with Cholera Toxin[1]

Ayako Wakabayashi, Yohko Nakagawa, Masumi Shimizu, Keiichi Moriya, Yasuhiro Nishiyama, and Hidemi Takahashi[2]

AQ: A **Priming of CTLs at mucosal sites, where various tumors are originated, seems critical for controlling tumors. In the present study, the effect of the oral administration of OVA plus adjuvant cholera toxin (CT) on the induction of Ag-specific mucosal CTLs as well as their effect on tumor regression was investigated. Although OVA-specific TCRs expressing lymphocytes requiring in vitro**
AQ: B **restimulation to gain specific cytotoxicity could be detected by OVA peptide-bearing tetramers in both freshly isolated intraepithelial lymphocytes and spleen cells when OVA was orally administered CT, those showing direct cytotoxic activity without requiring in vitro restimulation were dominantly observed in intraepithelial lymphocytes. The magnitude of such direct cytotoxicity at mucosal sites was drastically enhanced after the second oral administration of OVA with intact whole CT but not with its**
AQ: C **subcomponent, an A subunit (CTA) or a B subunit (CTB). When OVA plus CT were orally administrated to C57BL/6 mice bearing OVA-expressing syngeneic tumor cells, E.G7-OVA, in either gastric tissue or the dermis, tumor growth was significantly suppressed after the second oral treatment; however, s.c. or i.p. injection of OVA plus CT did not show any remarkable suppression. Those mucosal OVA-specific CTLs having direct cytotoxicity expressed CD8$\alpha\beta$ but not CD8$\alpha\alpha$, suggesting that they originated from thymus-educated cells. Moreover, the infiltration of such OVA-specific CD8$^+$ CTLs was observed in suppressed tumor tissues. These results indicate that the growth of ongoing tumor cells can be suppressed by activated CD8$\alpha\beta$ CTLs with tumor-specific cytotoxicity via an orally administered tumor Ag with a suitable mucosal adjuvant.** *The Journal of Immunology,* **2008, 180: 0000–0000.**

Many malignant tumors originate from various epithelial tissues such as the skin or mucosal sites such as the esophagus, stomach, colon, or lung (1). Thus, as a cancer vaccine, it is essential to stimulate mucosal or dermal immune systems, as well as the systemic immune system, with a suitable Ag, adjuvant, and administration route as reviewed by Finn (2). Mucosal immunization using an adjuvant that enables the priming of both mucosal and systemic immunity (3, 4) may be a good way to prevent or treat mucosal tumors. In particular, the induction of mucosal CTLs that can specifically recognize tumor-derived peptide Ags presented by the corresponding class I MHC molecules seems to be one of the most important issues for eliminating tumor cells (5).

AQ: D In the mucosal compartment, lymphocytes located between the intestinal epithelia are almost exclusively T cells called intraepithelial lymphocytes (IELs)[3] (3). Such IELs are mostly CD8$^+$ T cells that are classified into three distinct populations: TCR$\alpha\beta^+$ CD8$\alpha\beta^+$, TCR$\alpha\beta^+$CD8$\alpha\alpha^+$, and TCR$\gamma\delta^+$CD8$\alpha\alpha^+$ (6). IELs contain cytotoxic properties and specifically eliminate virus- or parasite-infected cells (7–9); however, although spontaneous cytotoxicity of human IELs against tumor cells has been reported (10, 11), their actual specificity on tumors is still unknown. Recently, we have reported (12) that a marked increase in the number of HIV-1-specific CD8$\alpha\beta$-positive T cells among IELs was observed in HIV-1-specific TCR transgenic (Tg) mice when they received intrarectal or i.p. administration of the recombinant vaccinia virus (rVV) expressing a known restricted CTL epitope, P18 (rVV-P18), which is restricted by H-2D^d-class I MHC molecules (13). Using H-2D^d/P18 tetramers, we could detect CD8-positive, AQ: E P18-specific TCR-expressing T cells in freshly isolated IELs and splenic T cells of unchallenged naive Tg mice. Although those H-2D^d/P18 tetramer-positive CD8 T cells from naive Tg mice did not show any specific cytotoxicity, freshly isolated mucosal T cells bearing CD8$\alpha\beta$ but not CD8$\alpha\alpha$ from activated Tg mice with rVV-P18 represented P18-specific cytotoxicity against tumor cells expressing the epitope, and the magnitude of cytotoxicity was much stronger than that in activated splenic T cells (12). These results suggest that in vivo activated mucosal CD8$\alpha\beta$ CTLs with tumor-specific cytotoxicity may be critical for controlling tumors expressing the specific epitope in vivo rather than systemic splenic CTLs.

Cholera toxin (CT) derived from *Vibrio cholerae* is known as a potent mucosal adjuvant comprised of one toxic A subunit (CTA) with ADP-ribosyltransferase activity and five nontoxic B subunits (CTB) responsible for binding to monosialoganglioside (GM) 1 on the cell surface (14, 15). CT adjuvant helps to produce both systemic IgG and mucosal IgA (16) as well as to induce Ag-specific

Department of Microbiology and Immunology, Nippon Medical School, Tokyo, Japan

Received for publication April 13, 2007. Accepted for publication January 7, 2008.

The costs of publication of this article were defrayed in part by the payment of page charges. This article must therefore be hereby marked *advertisement* in accordance with 18 U.S.C. Section 1734 solely to indicate this fact.

[1] This work was supported in part by Grants-in-Aid for Young Scientists from the Japan Society for the Promotion of Sciences, from the Ministry of Education, Science, Sport, and Culture, from the Ministry of Health and Labor and Welfare, Japan, and from the Promotion and Mutual Aid Corporation for Private Schools of Japan.

[2] Address correspondence and reprint requests to Dr. Hidemi Takahashi, Department of Microbiology and Immunology, Nippon Medical School, 1-1-5 Sendagi, Bunkyo-ku, Tokyo 113-8602, Japan. E-mail address: htkuhkai@nms.ac.jp

[3] Abbreviations used in this paper: IEL, intraepithelial lymphocyte; CT, cholera toxin; CTA, CT A subunit (toxic); CTB, CT B subunit (nontoxic); DC, dendritic cell; GM, monosialoganglioside; *Hp*, *Helicobacter pylori*; LPL, lamina propria lymphocyte; MadCAM-1, mucosal addressin cell-adhesion molecule-1; OVA-CT, CT-conjugated OVA; PP, Peyer's patch; rVV, recombinant vaccinia virus; SC, spleen cell; Tg, transgenic; TIL, tumor-infiltrating lymphocyte.

$CD4^+$ T cell responses in the spleen, reflecting the systemic compartment, and in Peyer's patches (PPs), reflecting the mucosal compartment (17). In addition, it has been demonstrated (18) that OVA-specific CTLs could be primed in C57BL/6 mice following oral exposure to a combination of OVA with CT, and specific cytotoxic activity was detected from spleen cells (SCs) only when they were restimulated in vitro with irradiated OVA-expressing syngeneic tumor cells, E.G7-OVA, which are OVA gene-transfected EL4 thymoma cells (19, 20). Also, intranasal preimmunization with OVA peptide (SIINFEKL) plus CT primed similar OVA-specific CTLs in the spleen of C57BL/6 mice, and the immunized mice were protected from the development of transferred E.G7-OVA (21).

Moreover, it has been shown that adoptive transfer of naive $CD8^+$ OVA-specific OT-I T cells into E.G7-OVA tumor-bearing syngeneic mice did not inhibit tumor growth, although adoptive transfer of preactivated OT-I CTL in vitro inhibited tumor growth in a dose-dependent manner (22). Furthermore, it has recently been reported that vaccination with dendritic cells (DCs) prepulsed ex vivo with CT-conjugated OVA (OVA-CT) gave rise to OVA-specific splenic $CD8^+$ T cells that produced IFN-γ, were cytotoxic to E.G7-OVA cells in vivo, and rejected already established in vivo E.G7-OVA tumors associated with high numbers of tumor-infiltrating $CD8^+$ T cells (23), indicating that the elimination of previously established tumor cells might require the infiltration of tumor-specific activated $CD8^+$ CTLs.

AQ: F

In the present study, we found two distinct types of $CD8\alpha\beta$-positive T cells among freshly isolated lymphocytes expressing OVA-specific TCRs, which can be detected by OVA peptide-bearing tetramers. One is in an activated effector state with cytotoxic activity and the other is a resting state and may gain cytotoxicity when stimulated with an OVA epitope peptide in vitro. Based on the observations, we defined direct cytotoxicity as the former state, in which freshly isolated and unstimulated CD8 T cells had specific cytotoxicity. Therefore, by comparing systemic SCs, we asked whether OVA-specific cytotoxic activity could be observed among freshly isolated IELs in mice orally administered OVA plus CT and examined whether those activated CTLs would reject or suppress the growth of already established tumors. Consequently, we observed dominant $TCR\alpha\beta$ and $CD8\alpha\beta$ OVA-specific CTL activities in freshly isolated IELs rather than in SCs after the oral administration of OVA plus CT, and such mucosal CTL activities could be expanded after oral boosting. Moreover, the growth of E.G7-OVA inoculated into the stomach or the epidermis was significantly suppressed, accompanied by the expansion of activated mucosal CTLs, and the infiltration of such OVA-specific $CD8\alpha\beta^+$ CTLs was observed in suppressed dermal tumor tissues. These results indicate that the growth of ongoing tumor cells can be suppressed in vivo by activated $CD8\alpha\beta$ CTLs with tumor-specific cytotoxicity via an orally administered tumor Ag with a suitable mucosal adjuvant.

Materials and Methods

Mice

Six- to 8-wk-old female C57BL/6 ($H\text{-}2^b$) mice were purchased from Charles River Japan, maintained in microisolator cages under pathogen-free conditions, and fed autoclaved laboratory chow and water. All animal experiments were performed according to guidelines for the care and use of laboratory animals set by the National Institutes of Health (NIH; Bethesda, MD) and approved by the Review Board of Nippon Medical School (Tokyo, Japan).

Oral and systemic immunization

Chicken egg OVA, grade V (Sigma Aldrich), was dissolved in sterilized PBS. Mice were orally administered 100 mg of OVA or 10 μg of CT (List Biological Laboratories) alone or 100 mg of OVA plus 10 μg of CT, CTA, or CTB (List Biological Laboratories) in 0.3 ml of PBS. In some experiments, mice were orally administered 10 mg of OVA plus 10 μg of CT. For systemic immunization, mice were i.p. or s.c. injected with 100 mg of OVA or the same dose of OVA plus 10 μg of CT.

Preparation of IELs, lamina propria lymphocytes (LPLs), SCs, and tumor-infiltrating lymphocytes (TILs)

IELs were prepared by the method described previously (12). In brief, after the small intestine, large intestine, or stomach was obtained from mice, fecal materials were flushed from the lumen with HBSS (Invitrogen Life Technologies) and connective tissues were carefully removed. The obtained guts were inverted and cut into several segments that were transferred to a 50-ml conical tube (Becton Dickinson Labware) containing 45 ml of HBSS with 5% FCS, 100 U/ml penicillin (Invitrogen Life Technologies), and 100 μg/ml streptomycin (Invitrogen Life Technologies). The tube was then shaken at 37°C for 45 min (horizontal position; orbital shaker at 150 rpm). Harvested cells from the intestinal epithelium were passed through a 10-ml syringe column containing loosely packed glass wool to remove tissue debris. Subsequently, the cells were suspended in 30% Percoll solution (Amersham Biosciences) and centrifuged for 20 min at 1,800 rpm. Cells at the bottom of the solution were then subjected to Percoll discontinuous gradient centrifugation for 20 min at 1,800 rpm and IELs were recovered at the interphase of 44 and 70% Percoll solutions. LPLs were prepared by the method described previously (24). In brief, after the small intestine, large intestine, or stomach was dissected from mice, fecal material was flushed from the lumen with HBSS and PPs were carefully removed. The obtained guts were inverted and cut into several segments that were transferred to a 50-ml conical tube containing 45 ml of HBSS with 5% FCS and 1 mM EDTA (Wako Pure Chemical Industries). The tube was shaken at 37°C for 45 min (horizontal position; orbital shaker at 150 rpm). The gut segments were then washed with PBS and shaken in 40 ml of HBSS with 5% FCS and 0.1 mg/ml collagenase (Sigma-Aldrich) at 37°C for 45 min (horizontal position; orbital shaker at 60 rpm). Harvested cells were passed through a nylon mesh and suspended in 40% Percoll solution, and then 70% Percoll solution was underlain. The solution was centrifuged for 20 min at 1,800 rpm and LPLs were recovered at the interphase of 40 and 70% Percoll solutions. These procedures provided >95% viable lymphocytes with a cell yield of $5–10 \times 10^6$ of small intestinal IELs, $2–3 \times 10^5$ of large intestinal IELs, $7–12 \times 10^3$ of gastric IELs, $4–9 \times 10^6$ of small intestinal LPLs, $1–3 \times 10^5$ of large intestinal LPLs, or $5–9 \times 10^4$ of gastric LPLs per mouse. The cells were suspended in complete T cell medium (25) composed of RPMI 1640 medium (Sigma-Aldrich) supplemented with 2 mM L-glutamine (ICN Biomedicals), 1 mM sodium pyruvate (Invitrogen Life Technologies), 0.1 mM nonessential amino acid (Invitrogen Life Technologies), a mixture of vitamins (ICN Biomedicals), 1 mM HEPES (Invitrogen Life Technologies), 100 U/ml penicillin (Invitrogen Life Technologies), 100 μg/ml streptomycin (Invitrogen Life Technologies), 50 μM 2-ME (Sigma-Aldrich), and heat-inactivated 10% FCS. For TIL preparation, tumors were removed from mice, incubated in 1 mg/ml collagenase (Wako Pure Chemical Industries) with PBS at 37°C for 1 h, and crushed gently. TILs were prepared using Percoll solutions as described in the previous paragraph regarding IEL preparation. The spleen was aseptically removed and a single cell suspension was prepared. For osmotic hemolysis, single cells were suspended in 0.1× PBS and an equal amount of 2× PBS was added immediately. To enrich IELs, LPLs, and TILs from mice, the interface between the 40 and 70% Percoll solutions (26), in which NK cells and unfractionated SCs, which may also include NK cells, must be included, was collected.

AQ: G

Flow cytometry analysis

Cells were double-stained with PE-labeled $H\text{-}2K^b$/OVA tetramer-SIINFEKL (Beckman Coulter) or $H\text{-}2K^b$/PB1 tetramer-SSYRRPVGI (Medical & Biological Laboratories) and FITC-labeled anti-mouse TCRβ, CD8α (BD Pharmingen), or CD8β (Caltag Laboratories). Peptide PB1 703–711, SSYRRPVGI, for the control tetramer was derived from influenza virus (27). Dead cells were determined using 7-aminoactinomycin D viability dye (Beckman Coulter) and stained cells were analyzed by FACScan using the CellQuest program (BD Biosciences).

In vitro restimulation of SCs or IELs with E.G7-OVA

Lymphocytes were restimulated in vitro by the method described previously (19). Freshly isolated SCs (3×10^7) or IELs (3×10^7) were restimulated with 3×10^6 irradiated (20,000 rad) E.G7-OVA cells (19, 20) ($H\text{-}2^b$; American Type Culture Collection) in 10 ml of complete T cell medium per upright 25-cm^2 flask in 5% CO_2 at 37°C for 6 days. Six days later, the viability of the lymphocytes was 35–51% in SCs and 16–26% in IELs. The

in vitro restimulated cells were collected and their OVA-specific cytotoxicity was measured by the following procedure.

CTL assay

For the CTL assay, freshly isolated IELs, SCs, or TILs were used. Cytolytic activity was measured using a standard ^{51}Cr-release assay as previously described (12). In brief, various numbers of effector cells were incubated with 3×10^3 ^{51}Cr-labeled targets for 6 h at 37°C in 200 μl of RPMI 1640 medium containing 10% FCS in round-bottom 96-well cell culture plates (BD Biosciences). After incubation, the plates were centrifuged for 10 min at 330 × *g*, and 100 μl of cell-free supernatants were collected to measure radioactivity with a Packard Auto-Gamma 5650 counter (Hewlett-Packard Japan). Maximum release was determined from the supernatant of cells that had been lysed by the addition of 5% Triton X-100, and spontaneous release was determined from target cells incubated without added effector cells. The percentage of specific lysis was calculated as 100 × (experimental release − spontaneous release)/(maximum release − spontaneous release). SEs of the means of triplicate cultures were always <5% of the mean. Each experiment was performed at least three times.

Measurement of in vivo antitumor effects

E.G7-OVA cells (5×10^6), OVA gene-transfected EL4 thymoma cells (19, 20), were implanted into the gastric or dermal tissue of syngeneic C57BL/6 mice (H-2^b). For tumor implantation into the gastric tissue, mice were anesthetized and underwent an abdominal operation and then E.G7-OVA cells in 50 μl of RPMI 1640 were injected into the muscle layer of the stomach using a syringe with a 29-gauge needle (Terumo). For implantation into the dermal tissue, mice were anesthetized and E.G7-OVA cells in 100 μl of RPMI 1640 were injected intradermally by a 29-gauge needle syringe. On day 3 after implantation into the gastric or dermal tissue, when the tumor mass became visible, tumor-bearing mice were orally or systemically administered OVA plus CT as described above. Seven days after the first administration, some of the mice were similarly boosted with the same materials. The growing tumors implanted into the gastric or dermal tissues were followed by measuring the length (*a*) and width (*b*), and tumor volume (*V*) was calculated according to the formula $V = ab^2/2$ as reported previously (28). When the longer axis of each tumor was >20 mm, all mice were anesthetized and sacrificed according to the guidelines for the care and use of laboratory animals set by the NIH.

Histological analysis of tumor tissues

Freshly excised tumor tissues were embedded in Tissue-Tek OCT compound (Sakura Finetek) at −80°C. Tissue segments were sectioned at 6 μm using a cryostat. Sections were placed on a poly-L-lysine-coated glass slide, air dried, and then fixed in 10% formalin PBS for 5 min and stained with H&E. For immunohistochemical staining, sections were fixed in cold acetone for 5 min and incubated with blocking solution (Block-ace; Dainippon Pharmaceutical) for 30 min at 37°C and then incubated with biotin-conjugated rat anti-CD8β Ab (Caltag Laboratories) or control isotype-matched rat IgG2a Ab (Caltag Laboratories) overnight at 4°C. Endogenous peroxidase was quenched by incubation in 0.3% H_2O_2 and 0.1% NaN_3 in distilled water for 10 min. The sections were incubated with avidin-biotin peroxide complexes (Vectastain ABC kit; Vector Laboratories) followed by color reaction with a Vectastain diaminobenzidine substrate kit (Vector Laboratories).

Statistical analysis

Student's *t* test was used to determine the statistical significance of differences between groups in tumor growth. Data were considered significant at $p < 0.05$.

Results

Priming of OVA-specific CD8αβ-positive CTLs with direct cytotoxicity via oral administration with OVA plus CT

It has been reported that OVA-specific CTLs could be primed in C57BL/6 mice by oral or i.v. immunization with OVA plus CT together with nontoxic CTB, and specific cytotoxic activity was detected from immune SCs only when they were restimulated in vitro with irradiated OVA-expressing syngeneic tumor (E.G7-OVA) cells (18). It has also been shown that activated CTLs but not naive primed CTLs could represent antitumor responses in vivo (22). Similarly, we have recently observed in HIV-1-specific CTL-TCR transgenic mice that activated CTLs but not freshly isolated TCR-bearing CD8αβ-positive T cells showed specific cytotoxicity, and the most critical sites for activating TCR-bearing CD8αβ T cells were mucosal compartments when Tg mice were administered a specific Ag for TCR (12).

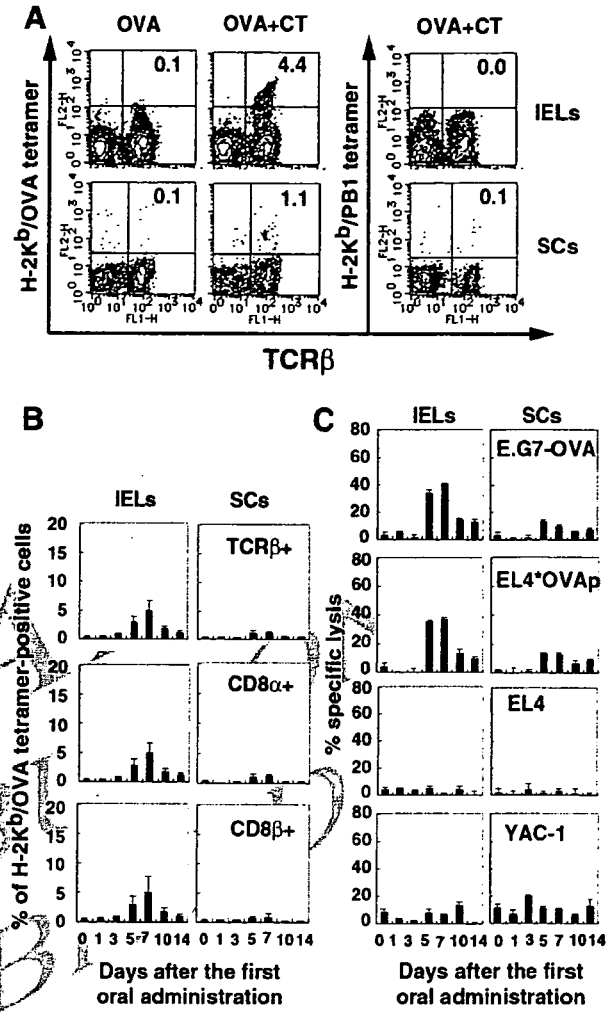

FIGURE 1. Analysis of OVA-specific direct cytotoxicities in IELs and SCs after primary immunization with OVA plus CT. *A*, Analysis of H-2K^b/OVA tetramer-positive cells. C57BL/6 mice were orally administered OVA or OVA plus CT once. IELs and SCs were collected from mice 5 days after the first oral administration, stained with either PE-labeled H-2K^b/OVA tetramer-SIINFEKL or H-2K^b/PB1 tetramer-SSYRRPVGI together with FITC-labeled anti-mouse TCRβ, and analyzed by flow cytometry. Each value represents the percentage of cells expressing both indicated markers. Data are representative of three independent experiments. *B*, Kinetics of H-2K^b/OVA tetramer-positive cells after primary immunization. C57BL/6 mice were orally administered OVA plus CT once. IELs and SCs were collected from mice at various days after the first oral administration, stained with PE-labeled H-2K^b/OVA tetramer together with FITC-labeled anti-mouse TCRβ, CD8α, or CD8β, and analyzed by flow cytometry. The results are shown as the mean ± SD of four mice. *C*, Kinetics of OVA-specific direct cytotoxic responses. C57BL/6 mice were orally primed and cells were collected as described in *B*. OVA-specific CTL responses were measured by ^{51}Cr-release assay using E.G7-OVA cells (H-2^b), YAC-1 cells, and EL4 cells (H-2^b) pulsed with or without 4 μM OVA-peptide, SIINFEKL, as target cells. E:T ratio was 100:1. The results shown as the mean ± SD in triplicate of pooled cells from two mice are representative of three independent experiments.

These findings prompted us to examine whether direct OVA-specific cytotoxic activity could be induced among IELs in mice

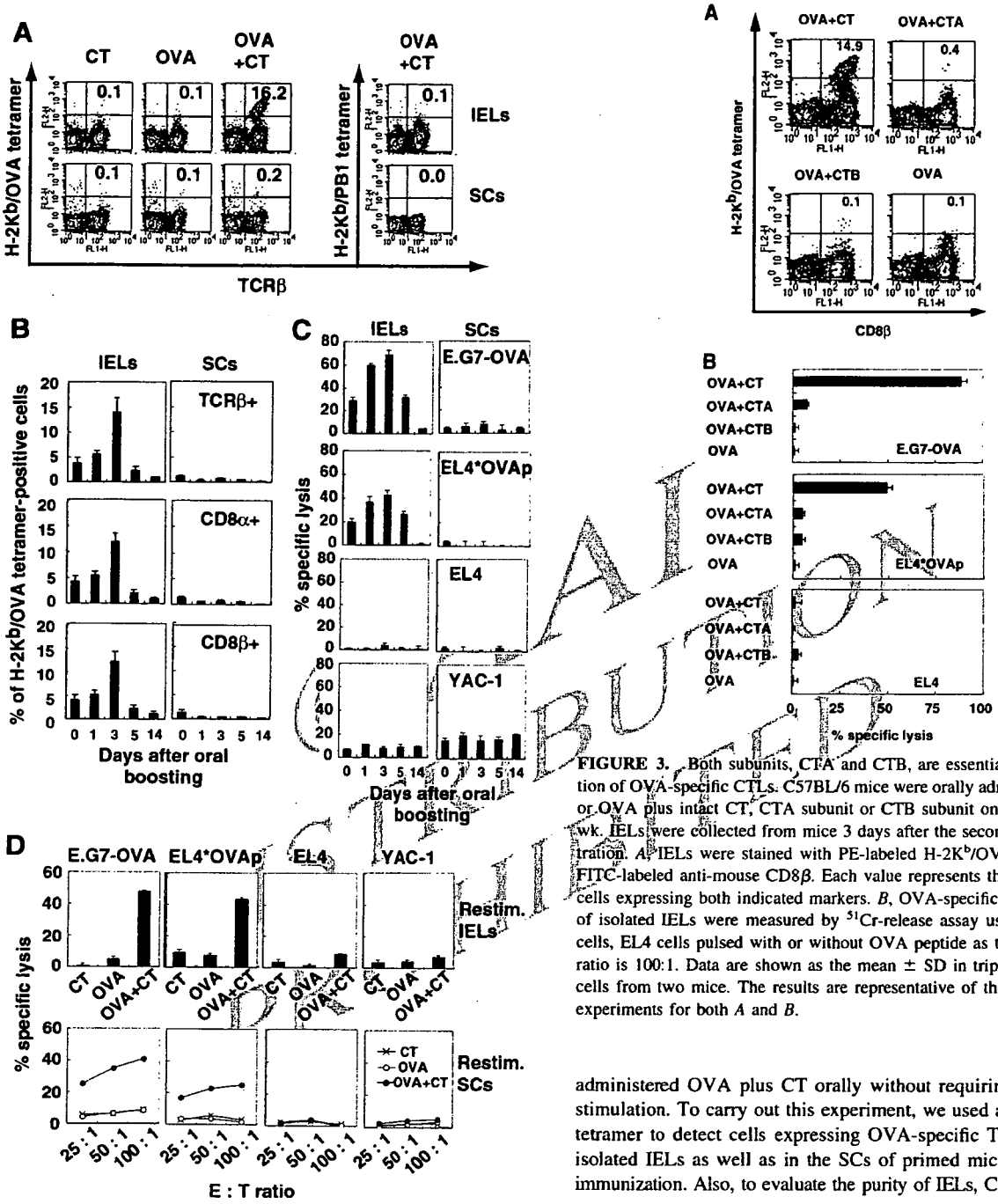

FIGURE 2. Expansion of direct OVA-specific cytotoxicities after oral boosting with OVA plus CT. *A*, Activated H-2K^b/OVA tetramer-positive cells after oral boosting. C57BL/6 mice were orally administered CT, OVA, or OVA plus CT once weekly for 2 wk. IELs and SCs were collected from mice 3 days after the second oral boost and stained with PE-labeled H-2K^b/OVA tetramer or H-2K^b/PB1 tetramer together with FITC-labeled anti-mouse TCRβ. Each value represents the percentage of cells expressing both indicated markers. Data are representative of three independent experiments. *B*, Kinetics of H-2K^b/OVA tetramer-positive cells after oral boosting. C57BL/6 mice were orally administered OVA plus CT once weekly for 2 wk. IELs and SCs were collected from mice at various days after the second oral boost, stained with PE-labeled H-2K^b/OVA tetramer together with FITC-labeled anti-mouse TCRβ, CD8α, or CD8β, and analyzed by flow cytometry. The results are shown as the mean ± SD of four mice. *C*, Kinetics of the secondary expansion of OVA-specific direct CTL responses. C57BL/6 mice were treated orally and the cells were collected as described in *B*. OVA-specific CTL responses were measured by ^{51}Cr-release assay using E.G7-OVA cells, YAC-1 cells, and EL4 cells pulsed with or without OVA peptide as targets. The E:T ratio is 100:1. The results shown as the mean ± SD in triplicate of pooled cells from two mice are representative of three independent experiments. *D*, Activation of OVA-specific CTLs by in vitro restimulation (Restim.). C57BL/6 mice were orally administered CT, OVA, or OVA plus CT once weekly for 2 wk. IELs (3×10^7) and SCs (3×10^7) were collected from mice 9 days after the second oral boost, and cocultured with 3×10^6 irradiated E.G7-OVA. Six days later, OVA-specific lysis of stimulated IELs and SCs was measured by ^{51}Cr-release assay. The E:T ratio is 100:1 in IELs and 100:1, 50:1, or 25:1 in SCs. The results are shown as the mean ± SD in IELs or the mean in SCs in triplicate of pooled cells from two mice. Data are representative of three independent experiments.

FIGURE 3. Both subunits, CTA and CTB, are essential for the induction of OVA-specific CTLs. C57BL/6 mice were orally administered OVA or OVA plus intact CT, CTA subunit or CTB subunit once weekly for 2 wk. IELs were collected from mice 3 days after the second oral administration. *A*, IELs were stained with PE-labeled H-2K^b/OVA tetramer and FITC-labeled anti-mouse CD8β. Each value represents the percentage of cells expressing both indicated markers. *B*, OVA-specific CTL responses of isolated IELs were measured by ^{51}Cr-release assay using E.G7-OVA cells, EL4 cells pulsed with or without OVA peptide as targets. The E:T ratio is 100:1. Data are shown as the mean ± SD in triplicate of pooled cells from two mice. The results are representative of three independent experiments for both *A* and *B*. AQ: P

administered OVA plus CT orally without requiring in vitro restimulation. To carry out this experiment, we used a H-2K^b/OVA tetramer to detect cells expressing OVA-specific TCR in freshly isolated IELs as well as in the SCs of primed mice 5 days after immunization. Also, to evaluate the purity of IELs, CD103 (integrin

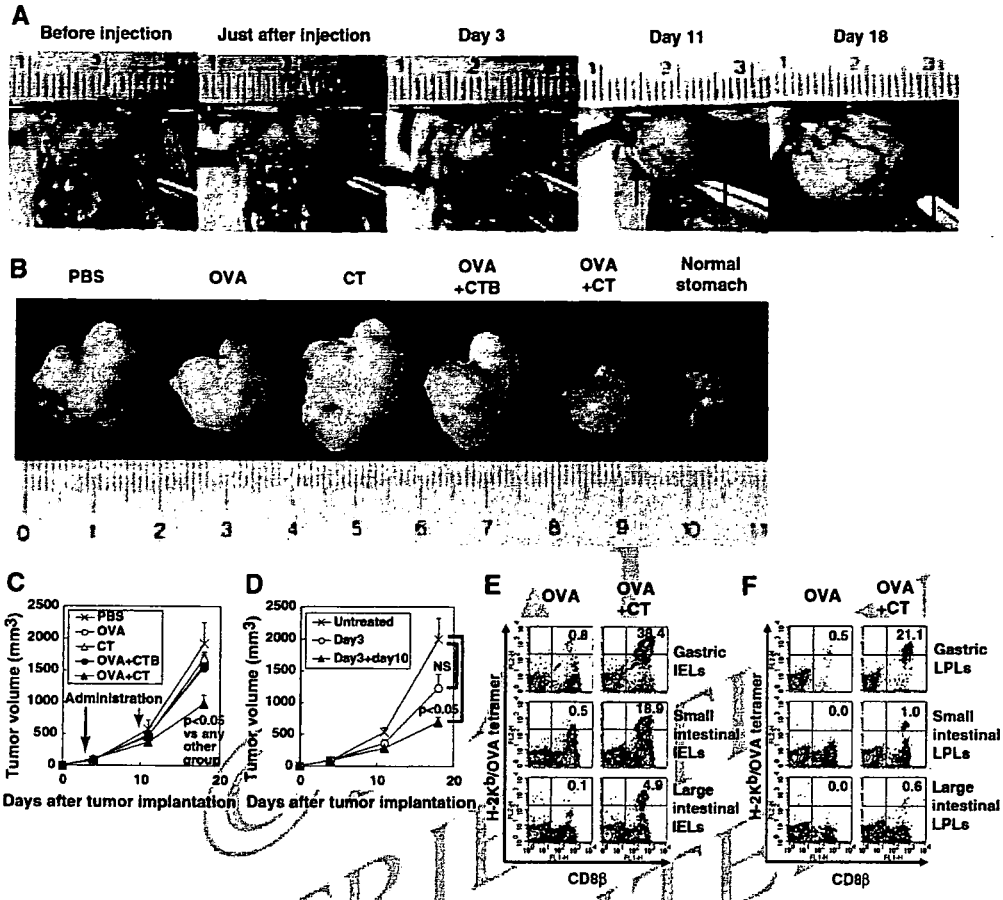

FIGURE 4. Suppression of the growth of a tumor implanted into gastric tissue by oral administration of OVA plus CT. *A*, Growth of visible tumor after implantation of E.G7-OVA cells into gastric tissue. C57BL/6 mice were implanted with 5×10^6 E.G7-OVA cells into the muscle layer of the stomach. Each day, the same mice were anesthetized and underwent an abdominal operation, and tumors were observed. Arrows point to both ends of the longer axis in the tumor. *B*, C57BL/6 mice were implanted with 5×10^6 E.G7-OVA cells into the muscle layer of the stomach. Three days later, tumor-bearing mice were orally administered PBS, OVA, CT, OVA plus CTB subunit, or OVA plus CT. Seven days later, the second oral administration was performed AQ: Q in the same manner. Stomachs were excised from the mice 18 days after tumor implantation, as well as from untreated, normal mice. *C*, Tumor volumes were calculated based on the formula described in *Materials and Methods*, and the results are shown as the mean ± SEM. The results were obtained from 9–13 mice per group. $p < 0.05$ indicates statistically significant difference between OVA plus CT (▲) and any other groups. *D*, C57BL/6 mice were implanted with E.G7-OVA cells in the stomach. Three days later, tumor-bearing mice were orally administered OVA plus CT or left untreated. Seven days later, some orally immunized mice were boosted in the same manner or left untreated. The results are shown as the mean ± SEM of 5–7 mice per group. $p < 0.05$ and NS indicate statistically significant and not significant differences, respectively, between the boosted (▲) and nonboosted (○) groups and the untreated group (×). *E* and *F*, Induction of CD8β and H-2K^b/OVA tetramer-positive cells in IELs (*E*) and LPLs (*F*) of the stomach, small intestine, or large intestine after oral administration of OVA plus CT. C57BL/6 mice were orally administered OVA or OVA plus CT once weekly for 2 wk. IELs and LPLs were collected from mice 3 days after the second oral administration. Cells were stained with PE-labeled H-2K^b/OVA tetramer and FITC-labeled anti-mouse CD8β. Each value represents the percentage of cells expressing both indicated markers. The results are representative of three independent experiments.

α-IEL chain)-positive cells in the collected samples were examined by flow cytometry. CD103 is highly expressed on >90% of IELs (29, 30) but on only 15% of SCs (31). In the present study, CD103-positive cells occupied >90% of IELs and ~15% of SCs (data not shown). Although a small number of OVA-specific TCR-expressing cells were detected in both IELs (4.5–5.0%) and SCs (1.0–1.5%) after oral administration of OVA plus CT in comparison with control H-2K^b/PB1-positive cells, H-2K^b/OVA tetramer-positive cells were not observed in mice treated with OVA alone F1 (Fig. 1*A*). Such OVA peptide-specific TCR-expressing cells were TCRγδ negative (data not shown) and both CD8α and β positive (Fig. 1*B*). The number of tetramer-positive cells, to which the magnitude of direct OVA-specific cytotoxicity closely corresponded, was maximal at day 7 after oral immunization with both IELs and SCs (Fig. 1*B*), but it did not correspond to NK cell activity as measured against YAC-1 targets (Fig. 1*C*). The results clearly AQ: J demonstrate that direct OVA-specific CTL cytotoxicity is dominantly observed in mucosal IELs after primary oral administration of OVA plus CT.

Augmentation and kinetics of direct OVA-specific cytotoxicity by CD8αβ CTLs among IELs and SCs via oral boosting with OVA plus CT at day 7 after the primary administration

As shown above, because only 4.5–5.0% of IELs were temporarily activated by a one-shot oral administration, we extensively examined the effect of oral boosting with OVA plus CT at various days after primary immunization. The number of H-2K^b/OVA tetramer-positive cells was significantly enhanced among IELs but not among SCs when primed mice were boosted (Fig. 2*A*). Such an F2 effect was highest when mice were boosted at day 7 after initial

priming (data not shown). Tetramer-positive cells were again
AQ: K TCRβ-, CD8α-, and CD8β-positive IELs and their number peaked at day 3 after boosting (Fig. 2*B*). Correspondingly, direct OVA-specific cytotoxicity was greatly enhanced among IELs and the maximal cytotoxicity of IELs was observed at day 3 after boosting (Fig. 2*C*), although such direct cytotoxicity appeared to be completely lost in SCs (Fig. 2*C*). Nonetheless, SCs showed good epitope-specific cytotoxicity similar to that of IELs when they were restimulated in vitro with irradiated E.G7-OVA (Fig. 2*D*), suggesting that the priming effect by the oral administration of OVA plus CT also remained in systemic SCs.

It should be noted that the memory of OVA-specific CTLs persisted among IELs but not SCs. When secondary boosting with OVA plus CT was performed even 6 mo after primary boosting at day 7, the number of H-2K^b/OVA tetramer-positive cells was still detected at ~6% in IELs, and they showed remarkable direct cytotoxicity of ~84.5% against E.G7-OVA cells and 58.4% against EL4 cells pulsed with OVA peptide 3 days after secondary boosting (data not shown). Again, we could not detect any measurable direct cytotoxicity in the SCs of secondary boosted mice (data not shown).

Both CTA and CTB subunits are required to induce direct OVA-specific cytotoxicity in IELs

CT is comprised of a single A subunit, CTA, and five B subunits, CTB. When OVA was administered orally to mice with either 10 μg of CTA or an equal amount of CTB, H-2K^b/OVA tetramer-positive cells as well as direct OVA-specific cytotoxicity could not
F3 be detected in IELs (Fig. 3, *A* and *B*) and SCs (data not shown), although a significant number of tetramer-positive cells and strong direct OVA-specific cytotoxicity were observed among IELs of mice administered orally with OVA plus 10 μg of intact CT (Fig. 3, *A* and *B*). Even when using 50 μg of CTA or CTB for the administration of OVA, direct cytotoxicity was not observed (data not shown); therefore, both CTA and CTB subunits are required to induce direct Ag-specific cytotoxicity.

Effects of oral administration and booting with OVA plus CT on OVA-expressing tumor growth established in the stomach

We then examined in vivo antitumor effects of oral administration with tumor Ag plus CT on already established tumors growing in mice. C57BL/6 mice were implanted with 5×10^6 syngeneic
F4 E.G7-OVA cells into the muscle layer of the stomach (Fig. 4*A*). Three days later, tumor-bearing mice (Fig. 4*A*) were orally administered various combinations of OVA plus adjuvant and boosted with the same materials 7 days after the initial oral administration. To our surprise, tumor growth in the stomach of mice orally administered OVA plus CT twice was visually (Fig. 4*B*) and significantly ($p < 0.05$; Fig. 4*C*) suppressed on day 18 after tumor implantation as compared with other control groups such as OVA plus CTB or CT alone. However, when tumor-bearing mice were orally administered OVA plus CT once and without boosting, no statistically significant suppression was observed on day 18 as compared with untreated control mice, although a slight suppressive effect could be seen (Fig. 4*D*). Therefore, two oral administrations of tumor-Ag plus CT with an appropriate interval induced significant ongoing tumor suppression.

As previously shown, direct OVA-specific cytotoxicity among small intestinal IELs was greatly enhanced after boosting with OVA plus CT (Fig. 2, *A*, *B*, and *C*). We also examined whether direct OVA-specific CTLs were induced in the IELs and LPLs of the stomach, small intestine, and large intestine from boosted mice in which gastric tumor growth was significantly suppressed. We observed an increase in the number of H-2K^b/OVA tetramer-positive

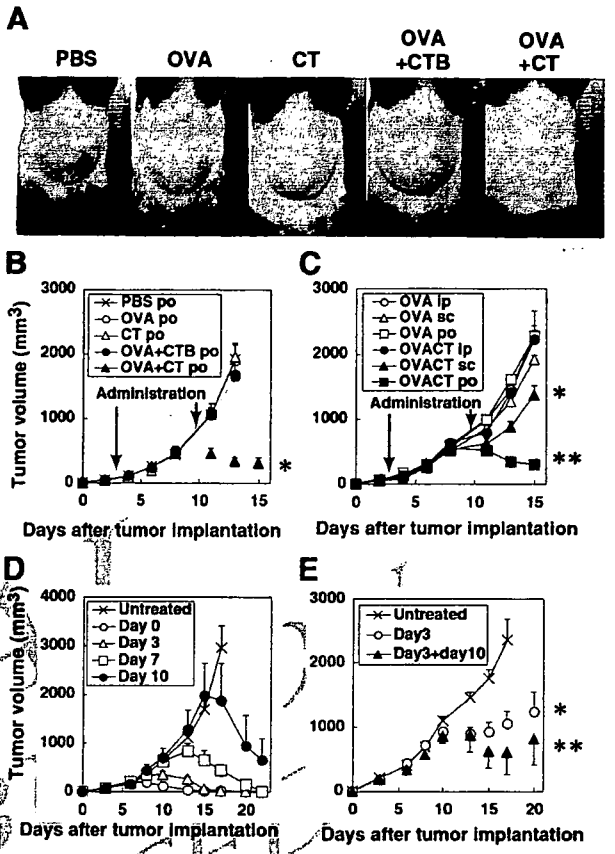

FIGURE 5. Suppression of intradermal tumor growth by oral administration with OVA plus CT. C57BL/6 mice were implanted intradermally with 5×10^6 E.G7-OVA cells. Three days later, tumor-bearing mice were orally administered PBS, OVA, CT, OVA plus CTB subunit, or OVA plus CT. Seven days later, the second oral administration was performed in the same manner. *A*, Visual suppressive effect of oral inoculation of OVA plus CT on dermal tumor growth. *B*, Tumor volumes were calculated based on the formula described in *Materials and Methods* and the results are shown as the mean ± SEM. Results were obtained from 5–6 mice per group. The asterisk (*) indicates statistically significant difference between the OVA plus CT group (closed triangle) and any other group at 11 days ($p < 0.05$) and 13 days ($p < 0.005$) after tumor inoculation. *C*, C57BL/6 mice were implanted intradermally with E.G7-OVA cells. Three days later, tumor-bearing mice were intraperitoneally (ip), subcutaneously (sc), or orally (po) administered OVA alone or OVA plus CT. Seven days later, the second treatment was performed in the same manner. The results are shown as the mean of tumor volumes ± SEM. Results were obtained from 5–6 mice per group. The asterisk (*) shows statistically significant differences ($p < 0.05$) between the s.c. OVA plus CT group (▲) and the s.c. OVA alone group at days 11, 13, and 15 after tumor implantation, and the two asterisks (**) indicate significant differences ($p < 0.01$) between the oral OVA plus CT group (■) and the oral OVA alone group on the same days. *D*, C57BL/6 mice were implanted intradermally with E.G7-OVA cells. The mice were orally administered once with OVA plus CT at day 0, 3, 7, or 10 after tumor implantation. The results are shown as the mean of tumor volumes ± SEM. Results were obtained from 10–12 mice per group. In single orally administered groups, significant tumor regression ($p < 0.05$) was observed at 7 days after oral administration compared with the untreated group. *E*, C57BL/6 mice were implanted intradermally with E.G7-OVA cells. Three days later, tumor-bearing mice were orally administered a low dose (10 mg) of OVA plus CT. Seven days later, some orally administered mice were boosted in the same manner. The results obtained from 5- mice per group are shown as the mean of tumor volumes ± SEM. The asterisk (*) indicates statistically significant differences ($p < 0.01$) between the nonboosted (○) and untreated mice (×) groups at days 15 and 17 after tumor implantation. and the two asterisks (**) indicate significant differences ($p < 0.005$) between the boosted (▲) and untreated groups on the same days.

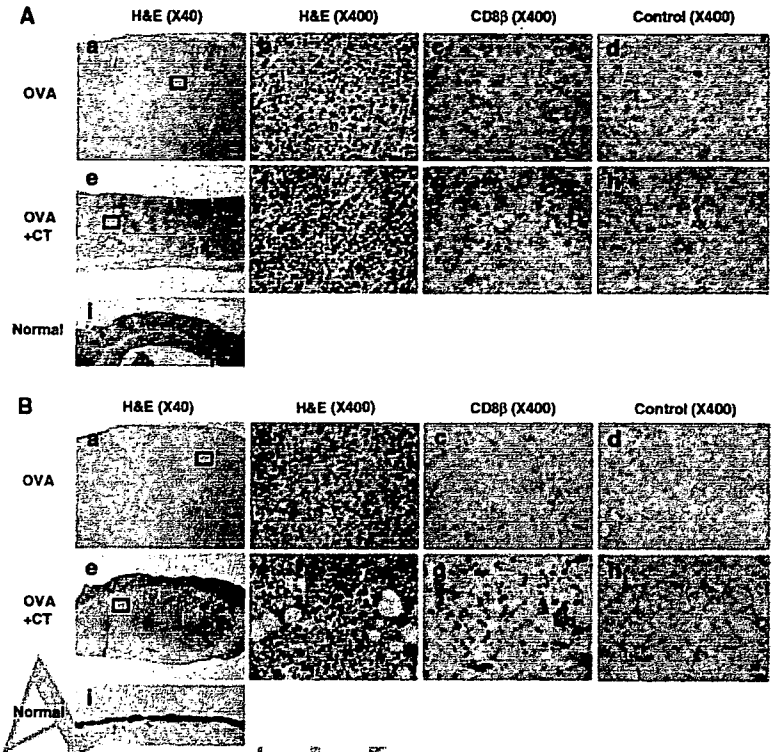

FIGURE 6. Infiltration of CD8$\alpha\beta$ positive lymphocytes into tumor tissues in mice orally administered OVA plus CT. C57BL/6 mice were implanted with 5×10^6 E.G7-OVA cells into the muscle layer of the stomach (*A*, *a–h*) or skin (*B*, *a–h*). Three days later, tumor-bearing mice were orally administered OVA (*A*, *a–d*, and *B*, *a–d*) or OVA plus CT (*A*, *e–h* and *B*, *e–h*). Seven days later, the second oral administration was performed in the same manner. Gastric and dermal tumor tissues were removed from mice 3 days after the second oral boost. Frozen sections of tumor tissues and normal tissues were prepared and stained with H&E (*A*, *a*, *b*, *e*, *f*, and *i* and *B*, *a*, *b*, *e*, *f*, and *i*) or immunohistochemically stained with biotin-conjugated rat anti-CD8β mAb (*A*, *c* and *g*, and *B*, *c* and *g*) or control isotype-matched rat IgG2a Ab (*A*, *d* and *h*, and *B*, *d* and *h*). Image magnification is either ×40 (*A*, *a*, *e*, and *i* and *B*, *a*, *e*, and *i*) or ×400 (*A*, *b–d* and *f–h* and *B*, *b–d* and *f–h*). *A*, *b* and *f* and *B*, *b* and *f* are enlarged images (×400) of the squared areas in the images (×40) of *A*, *a* and *e* and *B*, *a* and *e*, respectively.

cells among IELs in the stomach (38.4%) as well as the small (18.9%) and large intestine (4.9%) of tumor-suppressed mice (Fig. 4*E*) and also among LPLs in the stomach (21.1%) as well as the small (1.0%) and large (0.6%) intestine (Fig. 4*F*). Thus, the ability of LPLs to suppress tumor growth may be weaker than that of IELs. The results suggest that oral administration of Ag plus intact CT with appropriate mucosal boosting apparently suppressed the already established tumor growth in gastric tissue, particularly after oral boosting, probably through the activation of Ag-specific CTLs in the mucosal compartment.

Effects of oral administration and boosting with OVA plus CT on already established OVA-expressing dermal tumor growth

Next, we investigated the effect of the oral administration of tumor Ag plus CT on tumor growth in the skin, where the digestive tract is not directly associated. Mice were implanted with 5×10^6 E.G7-OVA cells intradermally. Three days later, tumor-bearing mice were orally administered various combinations of OVA plus adjuvant and boosted with the same materials 7 days after the initial oral administration. Interestingly, intradermal tumor growth was again strongly suppressed visually 11 days after tumor implantation in the dermis of mice orally administered OVA plus CT as compared with various other groups (Fig. 5*A*). This visual effect was confirmed by calculating the volume of the tumors established at day 11 and day 13 in each group ($p < 0.05$ and $p < 0.005$, respectively; Fig. 5*B*). We also examined the effect of the administration of tumor Ag plus CT via various routes on intradermal tumor growth. Although a slight suppression was observed by s.c. inoculation of OVA plus CT, tumor growth was not suppressed at all by i.p. administration in comparison with the oral treatment group (Fig. 5*C*). It should be noted that tumor growth in the dermis was markedly suppressed even by a single oral administration of OVA plus CT on day 0, 3, 7, or 10 after tumor implantation (Fig. 5*D*). In each group, tumor growth was suppressed ($p < 0.05$) and the tumor volume was small around 7 days after oral administration. Unexpectedly, there was almost no difference in the suppressive effects on tumor growth between mice treated with a single administration and boosted mice showing much stronger direct cytotoxicity (data not shown). However, when the dosage quantity of OVA was decreased by one-tenth, tumor growth in boosted mice was more significantly ($p < 0.005$) suppressed than in nonboosted mice ($p < 0.01$; Fig. 5*E*). Collectively, the results indicate that the oral administration of tumor Ag plus CT with appropriate mucosal boosting may induce a remarkable suppression of already established tumor growth in the skin via mucosally generated CTLs.

Infiltration of CD8$\alpha\beta$-positive cells in suppressed tumor tissues

We thus examined whether OVA-specific CD8$\alpha\beta$-positive CTLs were actually seen in suppressed tumor tissues such as the stomach and dermis. To determine tumor-infiltrating CD8$\alpha\beta^+$ cells, immunohistochemical staining was performed using biotin-conjugated rat anti-CD8β Ab (Fig. 6*A*, *c* and *g* and *B*, *c* and *g*) or control isotype-matched rat IgG2a Ab (Fig. 6*A*, *d* and *h* and *B*, *d* and *h*). Indeed, although mononuclear cells were seen in the gastric tumor tissues of mice treated with OVA alone, CD8$\alpha\beta$-positive cells were not observed at all (Fig. 6*A*, *a–d*). In contrast, infiltration of inflammatory mononuclear cells together with CD8$\alpha\beta$-positive cells was observed in suppressed gastric tumor tissues (Fig. 6*Ag*). As shown in Fig. 6*Ai*, normal gastric tissue is composed of the epithelium, lamina propria, lamina muscularis mucosae, muscle layer, and serosa from the inside surface in sequence. As compared with normal gastric tissue, a great number of large tumor cells (EG.7-OVA) were mainly found between the lamina muscularis mucosae and serosa of tumor-implanted tissues (Fig. 6*A*, *a* and *b*) and the infiltration of tumor cells into the lamina propria over the lamina muscularis mucosae was also observed (data not shown). However, in suppressed gastric tumor tissues (Fig. 6*Ae*) the tumor cell layer under the lamina muscularis mucosae was markedly thinner than that of an unsuppressed tumor (Fig. 6*Aa*), in which

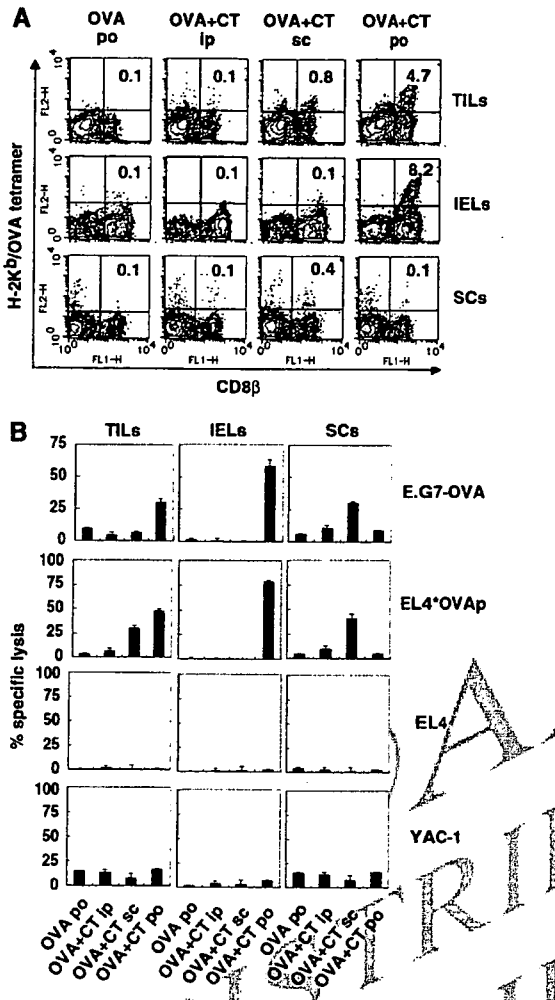

FIGURE 7. Detection of OVA-specific CTLs in TILs. C57BL/6 mice were implanted intradermally with E.G7-OVA cells. Three days later, mice were orally (po), subcutaneously (sc), or intraperitoneally (ip) administered OVA plus CT or orally treated with OVA. Seven days later, the second oral administration was performed in the same manner. TILs, IELs, and SCs were collected from mice 3 days after the second oral administration. *A*, TILs, IELs and SCs were double-stained with PE-labeled H-2K^b/OVA tetramer and FITC-labeled anti-mouse CD8β. *B*, OVA-specific CTL responses of TILs, IELs, and SCs were measured by a ^{51}Cr-release assay using E.G7-OVA cells, YAC-1 cells, and EL4 cells pulsed with or without OVA peptide as targets. The E:T ratio is 5:1 in TILs, or 100:1 in IELs and SCs. The results are shown as the mean ± SD in triplicate of pooled cells from three mice. The results are representative of three independent experiments.

tumor cells almost never infiltrated the lamina propria over the lamina muscularis mucosae. Similarly, as for dermal tumor tissues, mononuclear cells together with CD8αβ-positive cells were not observed in mice treated with OVA alone (Fig. 6*B*, *a–d*), whereas the infiltration of a large number of mononuclear cells and CD8αβ-positive cells was observed in suppressed dermal tumor tissues (Fig. 6*B*, *e–g*). Dermal tumor sections were not stained with control isotype-matched rat IgG (Fig. 6*B*, *d* and *h*). As shown in Fig. 6*Bi*, normal skin is composed of epidermides and dermis from the surface in sequence. In tumor cell-implanted dermal tissues, although the infiltration of mononuclear cells or CD8αβ-positive cells was not observed, many large tumor cells were found thickly beneath the epidermides (Fig. 6*B*, *a* and *b*); however, when tumor cell-implanted mice were treated with OVA plus CT, most tumor cells became necrotic or apoptotic (Fig. 6*B*, *e* and *f*).

Measurement of tumor-specific cytotoxic activity by tumor-infiltrating cells in tumor-suppressed mice

To confirm whether infiltrated CD8αβ-positive T cells achieved OVA-specific cytotoxicity, we isolated TILs containing both mononuclear cells and CD8αβ-positive T cells from suppressed dermal tumor tissues as well as from their IELs and SCs. As expected, the number of H-2K^b/OVA tetramer-positive cells increased in both the TILs and IELs but not in the SCs of mice bearing suppressed tumors induced by oral administration with OVA plus CT as compared with mice inoculated with OVA plus CT via another route (Fig. 7*A*), and those increased tetramer-positive cells showed significant direct OVA-specific CTL activity (Fig. 7*B*). It should be noted that, although the number of increased cells specific for the H-2K^b/OVA tetramer was small in mice inoculated with OVA plus CT s.c., both the TILs (0.8%) and the SCs (0.4%) but not the IELs (0.1%) of the mice represented a detectable level of direct OVA-specific cytotoxicity (Fig. 7*B*). These findings suggest that s.c. immunization with Ag plus CT may preferably activate systemic (splenic) Ag-specific CTLs rather than local (intraepithelial) CTLs. Moreover, NK cell cytotoxicity determined against YAC-1 cells was not observed in TILs, IELs, and SCs by oral, s.c., or i.p. immunization of OVA plus CT (Fig. 7*B*), indicating that the suppression of tumor growth was mainly mediated by CD8αβ CTLs rather than by NK cell cytotoxicity.

Discussion

In the present study we demonstrated that when OVA plus intact CT was orally administered into mice, direct OVA-specific cytotoxicity was dominantly induced in IELs rather than SCs after the first oral priming, and direct OVA-specific cytotoxicity was remarkably expanded in IELs but not in SCs after oral boosting with the same doses of OVA plus CT. Such OVA-specific CTLs were thymic conventional K^b class I MHC molecule-restricted TCRαβ$^+$ CD8αβ T cells (32). Moreover, the growth of the OVA-expressing tumor E.G7-OVA thymoma, established previously either in the stomach or dermis, was significantly suppressed by the oral administration of OVA plus CT. Furthermore, marked infiltration of OVA-specific TCRαβ$^+$ CD8αβ CTLs with direct cytotoxicity in reduced tumor tissues was observed. These results suggest that activated CTLs with specific cytotoxicity generated at mucosal compartments by oral administration with OVA plus intact CT may be responsible for already established tumor regression.

The majority of tumor regression studies associated with activation of the immune system have focused on systemic immunity observed in the spleen, lymph nodes, and circulating blood rather than local mucosal immunity seen in gut IELs. Those studies have demonstrated only preventative results for tumor establishment by preadministration of tumor Ag plus a suitable adjuvant. In addition, to our knowledge only one study has been shown to suppress already established tumor growth by activating and expanding tumor infiltrating CD8$^+$ CTLs (23). In that study, i.v. vaccination with DCs prepulsed ex vivo with OVA-CT at day 3 and boosted at day 10 after OVA-expressing E.G7 tumor injection induced complete rejection of a visible tumor within 3 wk after the first treatment. Although the inoculation route and the materials for vaccination were different from ours, the timing of the priming and boosting to induce the suppression of already established tumor growth correlated exactly, suggesting that their methods may also initiate strong mucosal direct cytotoxicity mediated through CD8$^+$ CTLs.

Similar to our findings, they also showed that immunization with OVA-CT but not with CTB-conjugated OVA (OVA-CTB)-prepulsed DCs could successfully induce complete rejection of already established tumor growth, although OVA-CTB-prepulsed DC inoculation prevented tumor establishment but not ongoing tumor growth in the skin. Moreover, they insisted that OVA has to be coupled to CT and should be loaded onto DCs for therapeutic DC vaccination based on the observation that neither OVA-CT nor DCs pulsed with unconjugated OVA plus CT could prevent tumor progression. Nonetheless, our findings shown here apparently indicate that we were able to induce effective suppression of ongoing tumor growth by simple oral administration with unconjugated OVA and CT. These results suggest that we may control already established tumor growth at the surface compartments by activating mucosal $CD8^+$ CTLs via orally administered tumor Ag with a suitable mucosal adjuvant. Also, when OVA-CT is orally administered, the conjugation between OVA and CT may be broken through digestion by enzymes secreted in the gastrointestinal tract. Recently, we have reported that modification of OVA in the gastrointestinal tract is essential for oral tolerance induction against OVA (33). Therefore, it is possible that gastrointestinal digestion or modification of OVA may facilitate the delivery of OVA Ag into DCs, critical APCs for OVA-specific CTL induction.

For the efficient induction of such OVA-specific CTLs in vivo using DCs, Eriksson et al. have reported that OVA-CT-prepulsed DC immunization required at least two DC injections, reflecting the priming/boosting procedure (23); however, we have observed that a single oral administration of OVA plus CT seems sufficient to induce effective CTLs to prevent E.G7-OVA thymoma growth, particularly in the skin. This may be because mucosally activated CTLs through oral immunization may be more potent than systemically activated CTLs to suppress transplanted tumors at the mucosal compartment, and oral administration of OVA plus CT seems more efficient to induce mucosal CTLs than i.v. Ag-loaded DC inoculation. Further studies will be needed to explain the differences.

Although both CT-conjugated OVA and CTB-conjugated OVA are cross-presented by MHC class I in DCs, only CT-OVA but not CTB-OVA cross-primes OVA-specific $CD8^+$ CTLs in vivo (23, 34). Additionally, DCs pulsed with intact OVA alone cannot cross-present and cross-prime CTLs (23). For the cross-priming of Ag-specific CTLs by Ag-captured immature DCs, maturation signaling via some surface molecules such as TLR-3 in those DCs is essential (35, 36). Although whole CT up-regulates the expression of MHC class II, B7.1, and B7.2 molecules on DCs in vitro, neither CTA nor CTB alone up-regulates the levels of surface markers on DCs (37, 38). Also, the binding of CTB to GM1 on DCs seems necessary to efficiently take up both CT itself and Ag and to induce cross-presentation by MHC class I molecules on DCs, whereas CTA may not be taken up to affect DCs. When DCs from GM1-lacking mice were matured in vitro, CT failed to up-regulate the expression of maturation markers and, thus, the binding of B subunits in CT to GM1 molecules on DCs is essential for the induction of DC maturation (37). It has been reported that CTA is required to not only assist in maturation but also to generate the migration of DCs (39, 40); therefore, CTB-mediated matured DCs can initiate their migration to secondary lymphoid organs and colocalization with naive T cells (38). Indeed, CT-loaded but not CTB-loaded DCs could migrate from marginal zones to T cell zones in the spleen (39) and from the subepithelial dome region to T cell zones in PPs (40); therefore, both CTA and CTB were essential for cross-priming CTLs in vivo and neither CTA nor CTB alone could induce CTLs at various compartments (Fig. 3). Taken together, although the detailed mechanisms of efficient Ag presentation via MHC class I and the maturation and migration of DCs by CT are still unknown, digested OVA might be efficiently captured by immature gut mucosal DCs in the presence of CTB and the captured Ag may be cross-presented by MHC class I during DC maturation and migration in the presence of CTA, resulting in the induction of mucosal class I MHC molecule-restricted CTLs that may cause the regression of previously established tumors.

$OVA\text{-}specific\ CD8^+$ CTLs were induced among not only the IELs but also the LPLs of the stomach, small intestine, and large intestine by oral administration of OVA plus CT, a higher percentage of OVA-specific CD8 CTLs was observed in the stomach, small intestine, and large intestine in order, and more specific CTLs were always detected among IELs than among LPLs (Fig. 4, *E* and *F*). Thus, CTLs are much easier to be induced in the upper and more superficial portions of the gastrointestinal tract when Ags are orally administrated with intact CT.

It has been reported that DCs in gastric mucosa are increased in *Helicobacter pylori* (*Hp*)-infected mice and that the response of DCs and T cells to *Hp* Ag is critical for *Hp*-induced gastritis (41). In the present study, Ag-specific CTLs in the stomach might be generated by mucosally activated DCs in the presence of CT and infiltrate-implanted gastric tumor tissues. It is possible that intestinally activated CTLs might migrate to the tumor-implanted stomach, which might also cause CTL infiltration. Actually, such effector CTLs usually express high levels of $\alpha_4\beta_7$ integrin and can home in to the gastric (42), and small and large intestinal mucosa (43) where mucosal addressin cell-adhesion molecule-1 (MadCAM-1), the ligand of $\alpha_4\beta_7$ integrin, is constitutively expressed by post-capillary endothelial cells in small (44, 45) and large intestinal lamina propria (46). Moreover, the number of gastric $\alpha_4\beta_7^{high}$ T cells increased markedly by oral administration of CT in mice (42). It has also been reported that MAdCAM-1 expression is increased in the gastric mucosa after oral administration with cholera vaccine composed of CTB and formalin-inactivated *V. cholerae* (47); therefore, MadCAM-1-expression in gastric mucosa and the recruitment of effector $\alpha4\beta7^{high}$ T cells to gastric mucosa might be enhanced by oral administration of the CT adjuvant and, thus, OVA-specific effector CTLs might efficiently infiltrate the OVA Ag-expressing tumor region in the stomach.

In the present study, we found that the growth of dermally implanted tumors was also suppressed by the oral administration of tumor Ag plus whole intact CT. The actual mechanisms for such suppression remains to be elucidated, but there are at least three distinct possibilities: first, the migration of Ag-specific CTLs from the gastrointestinal tract to the skin; second, the migration of Ag-presenting DCs activated in the mucosal compartments by CT; and third, the migration of both cells from the gastrointestinal tract to the skin at the same time. It has been reported that the levels of CCR4 expression, which is associated with T cell homing to the skin, are increased in gastric T cells by infection with *Hp* in humans (48). Moreover, mucosal DCs that take up Ag might migrate to regional lymph nodes near the dermal tumor and prime the CTLs there, and the CTLs could effectively infiltrate dermal tumor tissue. Indeed, Belyakov et al. demonstrated an opposite mechanism in which skin-derived DCs containing heat-labile enterotoxin of *Escherichia coli* migrated to PPs and induced mucosal CTLs by transcutaneous immunization of an Ag and CT (49). Although the detailed mechanisms of this migration of DCs between skin and mucosa are unknown, they have clearly shown that DCs can migrate between the mucosa and skin. We are currently comparing the alteration of DCs in the mucosal compartment, spleen, and lymph nodes after oral administration of an Ag plus natural CT.

Unfortunately, such natural CT is not an appropriate mucosal adjuvant for human clinical investigation (50); however, studies

using natural CT would provide important and critical information about the effect of CT that would be useful for mucosal immune activation. Based on the findings obtained by using natural CT in a mouse model system, we could establish much safer protocols with a mutant CT (51) that induces adenosine diphosphate ribosylation and cyclic adenosine monophosphate formation, which may prevent severe diarrhea as well as retain adjuvant properties. Taken together, an artificial CT-based vaccine targeting DCs may provide a strategy for efficient CTL induction and avirulent mucosal cancer vaccination.

Our data also indicate that E.G7-OVA tumor growth was suppressed by OVA-specific CTLs but not NK cells (Fig. 7*B*). Vaccination with OVA-CT-pulsed DC protects against E.G7-OVA tumor development in vivo in wild-type, NK-depleted, and CD4-deficient mice but not in CD8-deficient mice (34), indicating that the E.G7-OVA tumor might be controlled by CD8 T cells but not by NK cells or CD4 T cells. In fact, TILs in the suppressed tumor did not show any NK-related cytotoxicity (Fig. 7*B*). Moreover, it has been demonstrated that in vitro pretreatment of NK cells with CT inhibits NK cell killing of tumor (YAC-1 or P815), because G proteins in NK cell membranes are ADP ribosylated with CT and ribosylation inhibits the lysis of tumor cells (52); therefore, NK cells do not seem to be involved in the suppression of E.G7-OVA growth in vivo.

It has been shown that activated CTLs but not naive CTLs can represent antitumor (22) or antivirus (12) responses in vivo. In the present study, already established E.G7 tumor growth can be suppressed only when OVA-specific CTLs that show specific cytotoxicity without requiring in vitro restimulation are induced, particularly in the mucosal compartment. To our knowledge, this is the first demonstration of the visual suppression of already established tumor growth by the simple oral administration of tumor Ag plus mucosal adjuvant. The findings shown in the present study herald a new era for cancer immunotherapy.

Acknowledgments

We thank Dr. Yoshihiro Kumagai and Yoshihiko Norose for useful discussions and advice.

Disclosures

The authors have no financial conflict of interest.

References

1. Franks, L. M., and M. A. Knowles. 2005. What is cancer? In *Introduction to the Cellular and Molecular Biology of Cancer*, 4th Ed. M. A. Knowles and P. J. Selby, eds. Oxford University Press, New York, pp. 1–24.
2. Finn, O. J. 2003. Cancer vaccines: between the idea and the reality. *Nat. Rev. Immunol.* 3: 630–641.
3. Czerkinsky, C., F. Anjuere, J. R. McGhee, A. George-Chandy, J. Holmgren, M. P. Kieny, K. Fujiyashi, J. F. Mestecky, V. Pierrefite-Carle, C. Rask, and J. B. Sun. 1999. Mucosal immunity and tolerance: relevance to vaccine development. *Immunol. Rev.* 170: 197–222.
4. Yuki, Y., and H. Kiyono. 2003. New generation of mucosal adjuvants for the induction of protective immunity. *Rev. Med. Virol.* 13: 293–310.
5. Takahashi, H. 2003. Antigen presentation in vaccine development. *Comp. Immunol. Microbiol. Infect. Dis.* 26: 309–328.
6. Hayday, A., E. Theodoridis, E. Ramsburg, and J. Shires. 2001. Intraepithelial lymphocytes: exploring the third way in immunology. *Nat. Immunol.* 2: 997–1003.
7. Offit, P. A., and K. I. Dudzik. 1989. Rotavirus-specific cytotoxic T lymphocytes appear at the intestinal mucosal surface after rotavirus infection. *J. Virol.* 63: 3507–3512.
8. Chardes, T., D. Buzoni-Gatel, A. Lepage, F. Bernard, and D. Bout. 1994. *Toxoplasma gondii* oral infection induces specific cytotoxic CD8 $\alpha\beta^+$ Thy-1$^+$ gut intraepithelial lymphocytes, lytic for parasite-infected enterocytes. *J. Immunol.* 153: 4596–4603.
9. Muller, S., M. Buhler-Jungo, and C. Mueller. 2000. Intestinal intraepithelial lymphocytes exert potent protective cytotoxic activity during an acute virus infection. *J. Immunol.* 164: 1986–1994.
10. Taunk, J., A. I. Roberts, and E. C. Ebert. 1992. Spontaneous cytotoxicity of human intraepithelial lymphocytes against epithelial cell tumors. *Gastroenterology* 102: 69–75.
11. Roberts, A. I., S. M. O'Connell, L. Biancone, R. E. Brolin, and E. C. Ebert. 1993. Spontaneous cytotoxicity of intestinal intraepithelial lymphocytes: clues to the mechanism. *Clin. Exp. Immunol.* 94: 527–532.
12. Kuribayashi, H., A. Wakabayashi, M. Shimizu, H. Kaneko, Y. Norose, Y. Nakagawa, J. Wang, Y. Kumagai, D. H. Margulies, and H. Takahashi. 2004. Resistance to viral infection by intraepithelial lymphocytes in HIV-1 P18-I10-specific T-cell receptor transgenic mice. *Biochem. Biophys. Res. Commun.* 316: 356–363.
13. Takahashi, H., J. Cohen, A. Hosmalin, K. B. Cease, R. Houghten, J. L. Cornette, C. DeLisi, B. Moss, R. N. Germain, and J. A. Berzofsky. 1988. An immunodominant epitope of the human immunodeficiency virus envelope glycoprotein gp160 recognized by class I major histocompatibility complex molecule-restricted murine cytotoxic T lymphocytes. *Proc. Natl. Acad. Sci. USA* 85: 3105–3109.
14. Williams, N. A., T. R. Hirst, and T. O. Nashar. 1999. Immune modulation by the cholera-like enterotoxins: from adjuvant to therapeutic. *Immunol. Today* 20: 95–101.
15. Lencer, W. I., and B. Tsai. 2003. The intracellular voyage of cholera toxin: going retro. *Trends Biochem. Sci.* 28: 639–645.
16. Elson, C. O., and W. Ealding. 1984. Generalized systemic and mucosal immunity in mice after mucosal stimulation with cholera toxin. *J. Immunol.* 132: 2736–2741.
17. Marinaro, M., H. F. Staats, T. Hiroi, R. J. Jackson, M. Coste, P. N. Boyaka, N. Okahashi, M. Yamamoto, H. Kiyono, H. Bluethmann, et al. 1995. Mucosal adjuvant effect of cholera toxin in mice results from induction of T helper 2 (Th2) cells and IL-4. *J. Immunol.* 155: 4621–4629.
18. Bowen, J. C., S. K. Nair, R. Reddy, and B. T. Rouse. 1994. Cholera toxin acts as a potent adjuvant for the induction of cytotoxic T-lymphocyte responses with non-replicating antigens. *Immunology* 81: 338–342.
19. Carbone, F. R., and M. J. Bevan. 1989. Induction of ovalbumin-specific cytotoxic T cells by in vivo peptide immunization. *J. Exp. Med.* 169: 603–612.
20. Moore, M. W., F. R. Carbone, and M. J. Bevan. 1988. Introduction of soluble protein into the class I pathway of antigen processing and presentation. *Cell* 54: 777–785.
21. Porgador, A., H. F. Staats, S. Faiola, E. Gilboa, and T. J. Palker. 1997. Intranasal immunization with CTL epitope peptides from HIV-1 or ovalbumin and the mucosal adjuvant cholera toxin induces peptide-specific CTLs and protection against tumor development in vivo. *J. Immunol.* 158: 834–841.
22. Dalyot-Herman, N., O. F. Bathe, and T. R. Malek. 2000. Reversal of CD8$^+$ T cell ignorance and induction of anti-tumor immunity by peptide-pulsed APC. *J. Immunol.* 165: 6731–6737.
23. Eriksson, K., J. B. Sun, I. Nordstrom, M. Fredriksson, M. Lindblad, B. L. Li, and J. Holmgren. 2004. Coupling of antigen to cholera toxin for dendritic cell vaccination promotes the induction of MHC class I-restricted cytotoxic T cells and the rejection of a cognate antigen-expressing model tumor. *Eur. J. Immunol.* 34: 1272–1281.
24. Taguchi, T., J. R. McGhee, R. L. Coffman, K. W. Beagley, J. H. Eldridge, K. Takatsu, and H. Kiyono. 1990. Analysis of Th1 and Th2 cells in murine gut-associated tissues: frequencies of CD4$^+$ and CD8$^+$ T cells that secrete IFN-γ and IL-5. *J. Immunol.* 145: 68–77.
25. Takahashi, M., E. Osono, Y. Nakagawa, J. Wang, J. A. Berzofsky, D. H. Margulies, and H. Takahashi. 2002. Rapid induction of apoptosis in CD8$^+$ HIV-1 envelope-specific murine CTLs by short exposure to antigenic peptide. *J. Immunol.* 169: 6588–6593.
26. Semple, J. W., and M. R. Szewczuk. 1986. Natural killer cells in murine muscular dystrophy: IV. Characterization of Percoll fractionated splenic and thymic natural killer cells and natural killer-sensitive thymocyte targets. *Clin. Immunol. Immunopathol.* 41: 116–129.
27. Belz, G. T., W. Xie, and P. C. Doherty. 2001. Diversity of epitope and cytokine profiles for primary and secondary influenza a virus-specific CD8$^+$ T cell responses. *J. Immunol.* 166: 4627–4633.
28. Nakatsuka, K., H. Sugiyama, Y. Nakagawa, and H. Takahashi. 1999. Purification of antigenic peptide from murine hepatoma cells recognized by class-I major histocompatibility complex molecule-restricted cytotoxic T-lymphocytes induced with B7-1-gene-transfected hepatoma cells. *J. Hepatol.* 30: 1119–1129.
29. Kilshaw, P. J., and K. C. Baker. 1988. A unique surface antigen on intraepithelial lymphocytes in the mouse. *Immunol. Lett.* 18: 149–154.
30. Russell, G. J., C. M. Parker, K. L. Cepek, D. A. Mandelbrot, A. Sood, E. Mizoguchi, E. C. Ebert, M. B. Brenner, and A. K. Bhan. 1994. Distinct structural and functional epitopes of the α E β 7 integrin. *Eur. J. Immunol.* 24: 2832–2841.
31. Lefrancois, L., T. A. Barrett, W. L. Havran, and L. Puddington. 1994. Developmental expression of the α IEL β 7 integrin on T cell receptor γ δ and T cell receptor α β T cells. *Eur. J. Immunol.* 24: 635–640.
32. Rocha, B., P. Vassalli, and D. Guy-Grand. 1994. Thymic and extrathymic origins of gut intraepithelial lymphocyte populations in mice. *J. Exp. Med.* 180: 681–686.
33. Wakabayashi, A., Y. Kumagai, E. Watari, M. Shimizu, M. Utsuyama, K. Hirokawa, and H. Takahashi. 2006. Importance of gastrointestinal ingestion and macromolecular antigens in the vein for oral tolerance induction. *Immunology* 119: 167–177.
34. Sun, J. B., K. Eriksson, B. L. Li, M. Lindblad, J. Azem, and J. Holmgren. 2004. Vaccination with dendritic cells pulsed in vitro with tumor antigen conjugated to cholera toxin efficiently induces specific tumoricidal CD8$^+$ cytotoxic lymphocytes dependent on cyclic AMP activation of dendritic cells. *Clin. Immunol.* 112: 35–44.

35. Fujimoto, C., Y. Nakagawa, K. Ohara, and H. Takahashi. 2004. Polyriboinosinic polyribocytidylic acid [poly(I:C)]/TLR3 signaling allows class I processing of exogenous protein and induction of HIV-specific $CD8^+$ cytotoxic T lymphocytes. *Int. Immunol.* 16: 55–63.
36. Schulz, O., S. S. Diebold, M. Chen, T. I. Naslund, M. A. Nolte, L. Alexopoulou, Y. T. Azuma, R. A. Flavell, P. Liljestrom, and C. Reis e Sousa. 2005. Toll-like receptor 3 promotes cross-priming to virus-infected cells. *Nature* 433: 887–892.
37. Kawamura, Y. I., R. Kawashima, Y. Shirai, R. Kato, T. Hamabata, M. Yamamoto, K. Furukawa, K. Fujihashi, J. R. McGhee, H. Hayashi, and T. Dohi. 2003. Cholera toxin activates dendritic cells through dependence on GM1-ganglioside which is mediated by NF-κB translocation. *Eur. J. Immunol.* 33: 3205–3212.
38. Gagliardi, M. C., F. Sallusto, M. Marinaro, A. Langenkamp, A. Lanzavecchia, and M. T. De Magistris. 2000. Cholera toxin induces maturation of human dendritic cells and licences them for Th2 priming. *Eur. J. Immunol.* 30: 2394–2403.
39. Grdic, D., L. Ekman, K. Schon, K. Lindgren, J. Mattsson, K. E. Magnusson, P. Ricciardi-Castagnoli, and N. Lycke. 2005. Splenic marginal zone dendritic cells mediate the cholera toxin adjuvant effect: dependence on the ADP-ribosyltransferase activity of the holotoxin. *J. Immunol.* 175: 5192–5202.
40. Shreedhar, V. K., B. L. Kelsall, and M. R. Neutra. 2003. Cholera toxin induces migration of dendritic cells from the subepithelial dome region to T- and B-cell areas of Peyer's patches. *Infect. Immun.* 71: 504–509.
41. Drakes, M. L., S. J. Czinn, and T. G. Blanchard. 2006. Regulation of murine dendritic cell immune responses by *Helicobacter felis* antigen. *Infect. Immun.* 74: 4624–4633.
42. Michetti, M., C. P. Kelly, J. P. Kraehenbuhl, H. Bouzourene, and P. Michetti. 2000. Gastric mucosal $\alpha_4\beta_7$-integrin-positive CD4 T lymphocytes and immune protection against *Helicobacter* infection in mice. *Gastroenterology* 119: 109–118.
43. Lefrancois, L., C. M. Parker, S. Olson, W. Muller, N. Wagner, M. P. Schon, and L. Puddington. 1999. The role of β_7 integrins in CD8 T cell trafficking during an antiviral immune response. *J. Exp. Med.* 189: 1631–1638.
44. Berlin, C., R. F. Bargatze, J. J. Campbell, U. H. von Andrian, M. C. Szabo, S. R. Hasslen, R. D. Nelson, E. L. Berg, S. L. Erlandsen, and E. C. Butcher. 1995. α_4 integrins mediate lymphocyte attachment and rolling under physiologic flow. *Cell* 80: 413–422.
45. Berlin, C., E. L. Berg, M. J. Briskin, D. P. Andrew, P. J. Kilshaw, B. Holzmann, I. L. Weissman, A. Hamann, and E. C. Butcher. 1993. $\alpha_4\beta_7$ integrin mediates lymphocyte binding to the mucosal vascular addressin MAdCAM-1. *Cell* 74: 185–195.
46. Streeter, P. R., E. L. Berg, B. T. Rouse, R. F. Bargatze, and E. C. Butcher. 1988. A tissue-specific endothelial cell molecule involved in lymphocyte homing. *Nature* 331: 41–46.
47. Lindholm, C., A. Naylor, E. L. Johansson, and M. Quiding-Jarbrink. 2004. Mucosal vaccination increases endothelial expression of mucosal addressin cell adhesion molecule 1 in the human gastrointestinal tract. *Infect. Immun.* 72: 1004–1009.
48. Lundgren, A., C. Trollmo, A. Edebo, A. M. Svennerholm, and B. S. Lundin. 2005. *Helicobacter pylori*-specific $CD4^+$ T cells home to and accumulate in the human *Helicobacter pylori*-infected gastric mucosa. *Infect. Immun.* 73: 5612–5619.
49. Belyakov, I. M., S. A. Hammond, J. D. Ahlers, G. M. Glenn, and J. A. Berzofsky. 2004. Transcutaneous immunization induces mucosal CTLs and protective immunity by migration of primed skin dendritic cells. *J. Clin. Invest.* 113: 998–1007.
50. Clarke, L. L., B. R. Grubb, S. E. Gabriel, O. Smithies, B. H. Koller, and R. C. Boucher. 1992. Defective epithelial chloride transport in a gene-targeted mouse model of cystic fibrosis. *Science* 257: 1125–1128.
51. Yamamoto, S., Y. Takeda, M. Yamamoto, H. Kurazono, K. Imaoka, M. Yamamoto, K. Fujihashi, M. Noda, H. Kiyono, and J. R. McGhee. 1997. Mutants in the ADP-ribosyltransferase cleft of cholera toxin lack diarrheagenicity but retain adjuvanticity. *J. Exp. Med.* 185: 1203–1210.
52. Maghazachi, A. A., A. Al-Aoukaty, C. Naper, K. M. Torgersen, and B. Rolstad. 1996. Preferential involvement of Go and Gz proteins in mediating rat natural killer cell lysis of allogeneic and tumor target cells. *J. Immunol.* 157: 5308–5314.

Yutaka Takebe, Rie Uenishi, and Xiaojie Li

Laboratory of Molecular Virology and Epidemiology, AIDS Research Center,
National Institute of Infectious Diseases, Tokyo 162-8640, Tokyo, Japan

Global Molecular Epidemiology of HIV: Understanding the Genesis of AIDS Pandemic

I. Chapter Overview

Global dissemination of the *Human immunodeficiency virus* (HIV) represents a dramatic and deadly example of recent genome emergence and expansion. Since HIV-1 group M began its expansion in human population roughly 70 years ago (in early twentieth century), it has been diversifying rapidly, now comprising a number of different subtypes and

Advances in Pharmacology, Volume 56

1054-3589/08 $35.00
DOI: 10.1016/S1054-3589(07)56001-1

circulating recombinant forms (CRFs). Molecular epidemiological method has been useful tool to analyze the origin of HIVs and to track a course of global HIV dissemination. It could also provide the information critical to prevention and future vaccine strategies. In this chapter, we describe the classification and distribution of HIV genotypes and the biological and public health implications of genetic variability of this deadly pathogen.

II. Introduction

The HIV/AIDS pandemic continues to expand globally at a rate of 13,000 new infections everyday. The Joint United Nations Program on HIV/AIDS (UNAIDS) estimates that 40.3 (36.7–45.3) million individuals are living with HIV/AIDS, and about 25 million patients have already died (UNAIDS/WHO, 2005). A total of estimated 65 million individuals have been thus infected with HIV worldwide since the epidemic started a quarter century ago. In 2005 alone, there were 4.9 (4.3–6.6) million new HIV infections and 3.1 (2.8–3.6) million AIDS deaths (UNAIDS/WHO, 2005). This could be translated as that 9.3 new infections and 5.9 AIDS deaths occurred every minute (or a new infection every 6–7 sec and an AIDS death every 10 sec) worldwide. Figure 1 illustrates the magnitude of HIV/AIDS epidemic in different regions of the world.

Heterosexual transmission remains the dominant mode of transmission and accounts for ~85% of all HIV infections worldwide. Sub-Saharan Africa is an epicenter of the pandemic and continues to have high rates of new infections [3.2 (2.8–3.9) million per year]. It accounts for ~65% of new infections occurred worldwide in 2005 (Fig. 1). While HIV/AIDS epidemics came later in Asia, Asia is becoming the epicenter of second largest epidemic with ~1 million infections annually, accounting for 20% of new infections in the world (Fig. 1). Outside of Sub-Saharan Africa, one third of HIV infections are acquired through injecting drug use, most of which (an estimated 8.8 millions) are in Eastern Europe and central and Southeast Asia. The interplay between injecting drug use and unprotected sex fuels the epidemics in many countries in Asia (Fig. 1).

Molecular epidemiology has been a useful tool to analyze the origin of HIVs and to track a course of global HIV spread. The study areas include the distribution of HIV genotypes in different geographic areas, route of global and regional virus spread, molecular features of emerging epidemics and regional outbreaks, and specific association with different epidemiologic features, such as risk behaviors. Recent investigations also provide the new data on the role of recombination in the generation of HIV genetic diversity and the frequency of dual and superinfections. In this chapter, we overview the recent advances in the study of global molecular epidemiology of HIV and discuss its biological and public health implications.

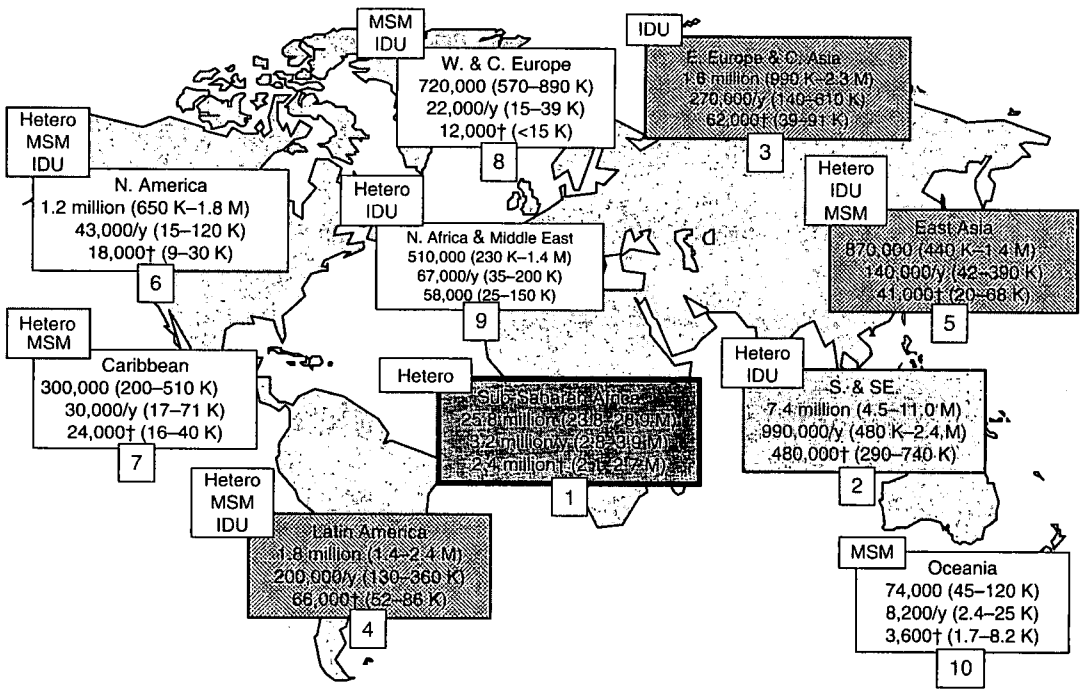

FIGURE 1 Distribution and estimated magnitude of HIV infections in different geographical regions of the world. UNAIDS/WHO estimates for the number of people living with HIV, people newly infected with HIV (/y) and AIDS death (†) in 2005 for the respective geographical regions are boxed. Predominant modes of transmission for each region are shown in the left upper box: Hetero, heterosexual; MSM, men who have sex with men; IDU, injecting drug user. Arabic numeral "1" in the box indicates the most afflicted region with the highest annual incidence and "10" indicates the least afflicted region. Global totals are shown at the bottom. Illustrations based on UNAIDS/WHO (2005).

III. Genotype Classification of HIVs

A. HIV Types (HIV-1 and HIV-2)

Etiologic agents for AIDS are subdivided into two related human retroviruses (lentiviruses): HIV-1 (HIV type 1) and HIV-2 (HIV type 2). HIV-1 is distributed worldwide, accounting for the majority of HIV infections. By contrast, HIV-2 is confined to West Africa and southern/western India (Schim van der Loeff *et al.*, 1999). Sporadic occurrences and transmission outbreaks of HIV-2 have been reported from many European countries (Cilla *et al.*, 2001; Damond *et al.*, 2004) and North and South America (Sullivan *et al.*, 1998) as well as Korea (Kim *et al.*, 2000; Nam *et al.*, 2006). It is known that the sexual and perinatal transmissions of HIV-2 are much less efficient than HIV-1 (Kanki *et al.*, 1994). This is attributed to a lower viral burden of HIV-2 during the relatively long asymptomatic period and may be the reason why the number of HIV-2-infected individuals has remained small, confined to limited geographic regions compared with HIV-1 infections (Schim van der Loeff *et al.*, 1999).

B. Genotype Classification of HIV-1s

Phylogenetic sequence analyses of HIV-1 strains distributed worldwide have identified three distinct groups of HIV-1 (M, N, and O), and nine genetic subtypes (A–D, F–H, J, and K) within major group (M) (Robertson *et al.*, 1999) (Fig. 2). The vast majority (more than 95%) of HIV-1 strains belong to group M (for Major or Main). Group O (for Outlier) comprises a pool of highly divergent, genetically related strains (Charneau *et al.*, 1994; Gurtler *et al.*, 1994; Loussert-Ajaka *et al.*, 1995; Vanden Haesevelde *et al.*, 1994) (Fig. 2). Group O infections are limited to people living in central Africa (Cameroon, Gabon, and equatorial Guinea), but even in this area they represent a small minority of HIV-1 infections. Only a few cases of group N (for New, or non-M/non-O) infections were identified in only limited number of patients from Cameroon (Simon *et al.*, 1998). HIV-1 group N infections fail to react serologically in standard whole-virus enzyme-linked immunosorbent assay (ELISA), yet are readily detectable by conventional Western blot analysis.

1. HIV-1 Subtypes

HIV-1 group M viruses are classified into at least nine discrete genetic subtypes (A–D, F–H, J, and K) based on the sequence of complete viral genomes (Fig. 2). In some subtypes, subclusters within subtypes were identified, leading to a classification into subsubtypes: The subtype F is subdivided into two subsubtypes: F1 and F2, and subsubtypes A1 and A2 strains were identified within subtype A (Fig. 2). The subtypes B and D are more

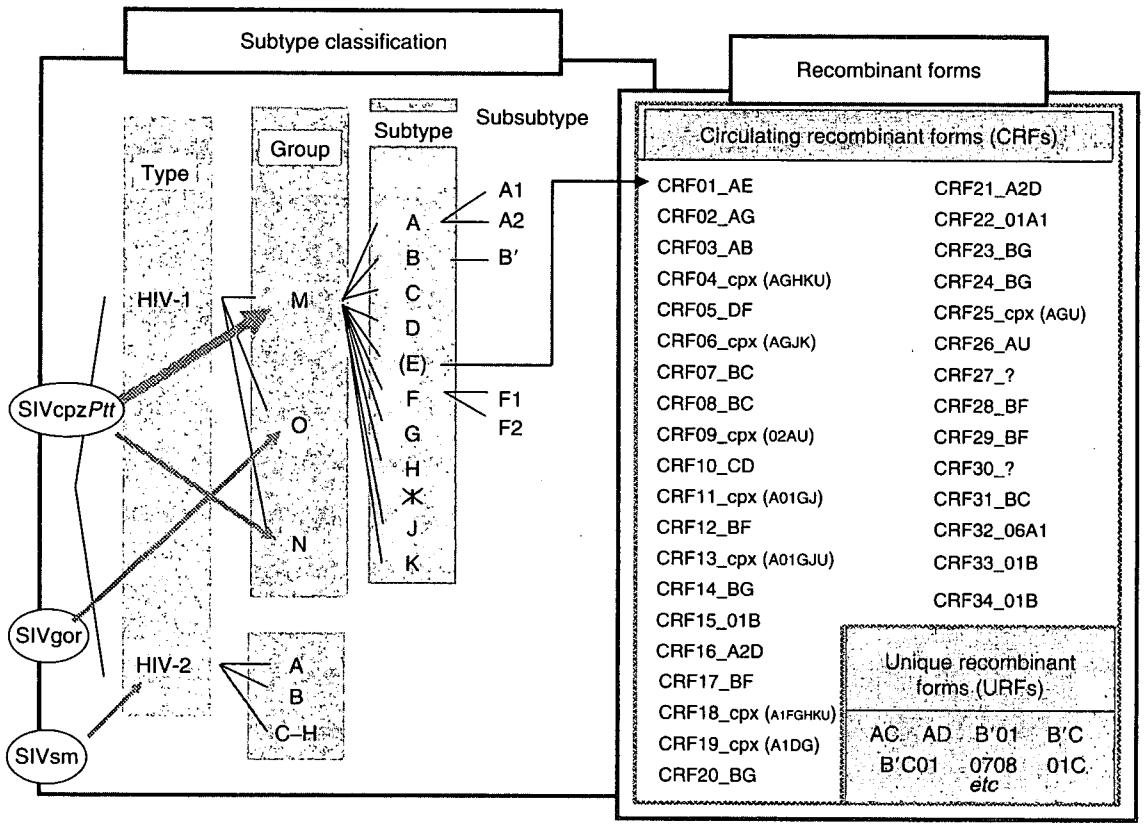

FIGURE 2 Classification of HIV genotypes and their origins. HIVs are classified based on the following four different strata: types (types 1 and 2), groups (M, O, and N for HIV-1; A–G for HIV-2), subtypes (A–K for HIV-1), and subsubtypes (A1 and A2, F1 and F2). HIV-1 recombinants in pandemic strains belonged to group M are categorized into circulating recombinant forms (CRFs) and unique recombinant forms (URFs) by their magnitude of dissemination. HIV-1 subtype B′ (B "prime") (Thailand variant of subtype B, also referred to as Thai-B), a unique regional subtype variant strongly associated with bloodborne transmission (prevalent among IDUs and former plasma donors/paid blood donors) in Southeast and East Asia. The plausible origins and routes of cross-species transmissions of HIVs are depicted in the left side (see text).

closely related to each other than to other subtypes, and therefore better considered as subsubtypes within a single subtype, rather than different subtypes. However, for the consistency with earlier published works, their original designation as subtypes is retained (Robertson *et al.*, 1999). Intrapatient genetic diversity of HIV-1 can vary from 6 to 10% in nucleotide sequence. HIV-1 isolates within a subtype may exhibit nucleotide distances of 15% in *gag* and up to 30% in *env* gp120-coding sequences. Intersubtype genetic diversity may range between 30 and 40%, depending on the gene analyzed. Similarly, the amino acid distances among different subtypes of HIV-1 group M reach ~25–30% in the *env* gene sequence and 15% in the *gag* gene sequence (Robertson *et al.*, 1999).

2. *HIV-1 Recombinants*

a. Circulating Recombinant Form It was realized that certain HIV-1 strains clustered with different subtypes in different regions of their genomes. Some of these mosaic HIV-1 genomes have been identified in several, apparently unlinked, individuals and play a major role in the global AIDS pandemic, designated as "CRFs" (Carr *et al.*, 1998). A total of 34 CRFs are currently recognized (http://hiv-web.lanl.gov/CRFs/CRFs.html) (Fig. 2). The global distribution of HIV genotypes are shown in Figs. 3 and 4. Under new nomenclature proposals, each CRF is designated by an identifying number, with letters indicating the subtypes involved. If the genome contains sequences originating more than two subtypes, the letters are replaced by "cpx," denoting "complex." To define a new subtype, subsubtype, or CRF, the representative strains must be identified in at least three epidemiologically unlinked individuals. Three near full-length genomic sequences are preferred, but two complete genome with partial sequences of a third strain are sufficient to designate a new subtype, subsubtype, or CRF (Robertson *et al.*, 1999).

b. Unique Recombinant Form In addition to CRFs, various types of "unique" recombinant forms (URFs) have been reported, currently without evidence of epidemic spread (McCutchan, 2000). URFs are diverse forms of HIV-1 intergenotype recombinants with unique mosaic structures, seen only in a single person or in a few epidemiologically linked individuals. Most of the URFs have been detected in the regions where multiple subtypes are cocirculating. A wide variety of URFs have been reported in the regions including Democratic Republic of Congo (DRC) (A/G/J and F1/K/U) (Vidal *et al.*, 2000), Tanzania (A1/C and A1/D) (Hoelscher *et al.*, 2001), Argentina (B/F) (Thomson *et al.*, 2000), Cuba (various combinations between subtypes A, B, D, G, and H) (Cuevas *et al.*, 2002), Spain (B/G) (Thomson *et al.*, 2001), India (A/C) (Lole *et al.*, 1999), Thailand (CRF01_AE/B) (McCutchan, 2000), Myanmar (various combinations between subtypes B′, C and CRF01_AE) (Motomura *et al.*, 2000, 2003; Takebe *et al.*, 2003), and China (B′/C) (Yang *et al.*, 2002, 2003 (Fig. 3). The detection of substantial

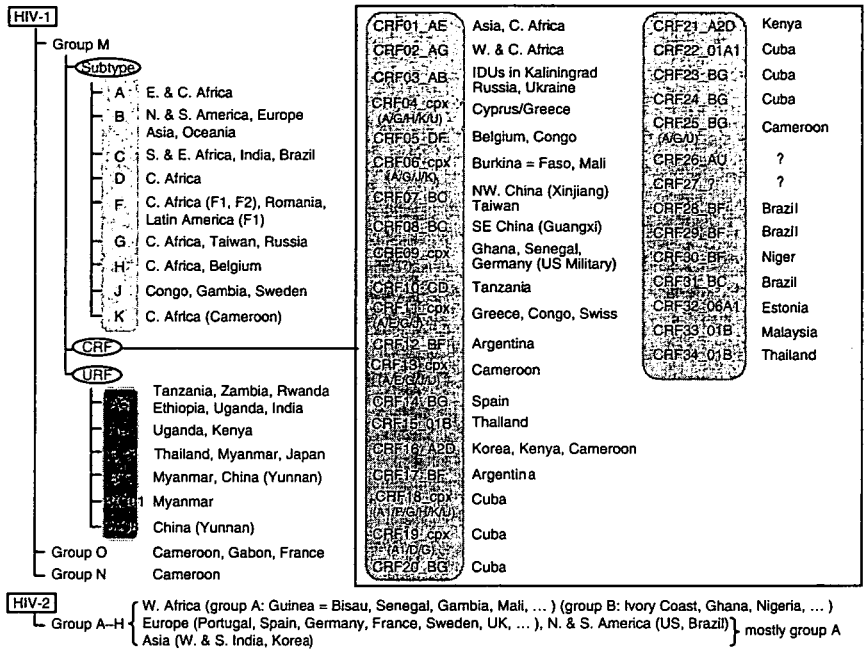

FIGURE 3 Geographical distribution of HIV genotypes. The global distributions of HIV-1 genotypes (groups, subtypes/subsubtypes, and CRFs/URFs) and HIV-2 groups are shown.

numbers of different URFs worldwide suggests that dual/multiple infections or superinfections with different lineages of HIV-1 strains might not be a rare event.

C. HIV-2: Genotype Classification and Geographic Distribution

HIV-2s are known to be members of a broader HIV-2/*Simian immunodeficiency virus* sooty mangabey (SIV-sm) phylogenetic group. HIV/SIV-sm phylogenetic groups are classified into eight genetic "groups" (A–H) (Damond *et al.*, 2004). Because these HIV-2 clades are nearly as distant from one another as are sequences from HIV-1 groups M, N, and O, HIV Nomenclature Committee decided to use "groups" rather than "subtypes" for HIV-2 genetic classification. Among these seven HIV-2 groups, only HIV-2 groups A and B are disseminated into significant numbers of human populations (Berry *et al.*, 2001; Schim van der Loeff *et al.*, 1999). HIV-2 group A has been identified predominantly in the western part of West Africa including Guinea, Bissau, Senegal, Gambia, and Mali. In contrast, HIV-2 subtype B has been found in central and eastern West African countries, including Ivory Coast, Ghana, and Nigeria.

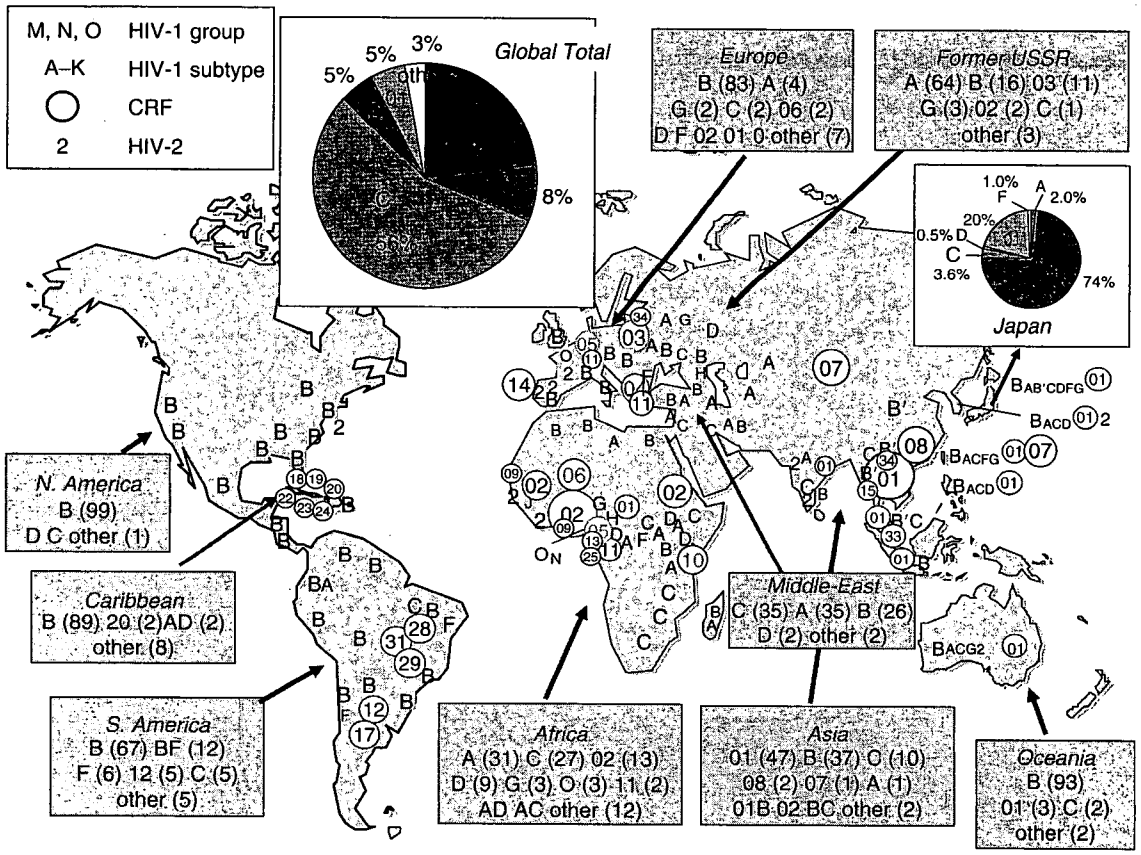

FIGURE 4 Global distribution of HIV genotypes and their estimated proportions. The number in parenthesis after each genotype is the proportion (in percentage) of the indicated genotype in the respective geographic regions. Data source (http://www.hiv.lanl.gov/components/hiv-web/new_geography/). A global total is adopted from Esparza and Bhamarapravati (2000). HIV-1 genotype distribution in Japan is also included. (See Color Plate Section.)

Outside of Africa, unique HIV-2 transmission focuses and clusters were observed in India and Korea. HIV-2 infections were reported in West and South India, frequently associated with dual infections of subtype C strains (Grez *et al.*, 1994; Pfutzner *et al.*, 1992). Ten cases of HIV-2 infections have been reported so far in Korea, where two distinct clusters of HIV-2 (group A) infections were recognized (Nam *et al.*, 2006). The index case (seamen) responsible for each cluster appears to be infected in West Africa and subsequently transmitted the virus to its sexual partners through heterosexual and homosexual contacts inside Korea. While most of the HIV-2 infection cases in Asia are the infections with HIV-2 group A, one HIV-2 group B infection was identified in a person with Korean nationality living in Japan (Kusagawa *et al.*, 2003), who was likely to be infected through heterosexual contacts in DRC (Nam *et al.*, 2006).

IV. Global Distribution of HIV Genotypes

A. Global HIV-1 Variability

On a global scale, the most prevalent HIV-1 genotypes are subtypes C (56%), A (23%), B (8%), D (5%), and CRF01_AE (5%) in 1999 (Esparza and Bhamarapravati, 2000) (Fig. 4). The greatest genetic diversity of HIV-1 has been found in central Sub-Saharan Africa. Subtypes A and C are most common, but all groups and subtypes have been identified. The extensive diversification of HIV-1 group M appears to occur within or near the DRC, where the highest diversity of group M has been recorded (Kalish *et al.*, 2004; Vidal *et al.*, 2000), and the earliest case of HIV-1 infection, dating back to 1959 (Zhu *et al.*, 1998), has been documented. It is consistent to the notion that central Sub-Saharan Africa is the likely origin of current pandemic. In South and East Africa, subtype C predominates (Novitsky *et al.*, 1999) that causes the worst epidemic in those regions with the adult HIV prevalence of more than 30%. In West and West central Africa, the majority of circulating strains is CRF02_AG (Carr *et al.*, 1998). Subtype B viruses remain the most prevalent isolates in North and South America, Western and Central Europe, and Australia, and are also common in several countries in Asia (Hongkong, Japan, Korea, and Taiwan), northern Africa, the Middle East, and among South African and Russian homosexual men. In South America, subtype B is prevalent, while subtypes F and C, and CRF12_BF (Thomson *et al.*, 2000) and other B/F recombinants (CRF17, 28 and 29_BF) (Thomson *et al.*, 2002) have been reported (Section IV.C).

B. HIV-1 Variants in Asia

Studies revealed unique profiles of HIV-1 genotype distribution in Asia. HIV-1 subtype C predominates in India (Lole *et al.*, 1999), with estimated